

**EXTRACTION AND CHARACTERIZATION OF MICRO  
FIBRILLATED CELLULOSE FROM TEXTILE COTTON  
WASTE**

**Jayasinghe Mudalige Ravisrini Jayasinghe**

**159483 A**

**Degree of Master of Science**

**Department of Materials Science and Engineering**

**University of Moratuwa.**

**Sri Lanka.**

**July 2020**

**EXTRACTION AND CHARACTERIZATION OF MICRO  
FIBRILLATED CELLULOSE FROM TEXTILE COTTON  
WASTE**

**Jayasinghe Mudalige Ravisrini Jayasinghe**

**159483 A**

**This Dissertation submitted in partial fulfillment of the requirements for the  
Degree of Master of Science in Material Science.**

**Department of Materials Science and Engineering**

**University of Moratuwa**

**Sri Lanka**

**July 2020**

## Declaration

I do herewith declare that the reported work in this entire thesis and the experiment was carried out by myself under the supervision of Mr. A. M. P. B. Samarasekara and Dr. D.A.S. Amarasinghe. This thesis describes the results of my own independent experimental work except where I have mentioned due references made in the text. There was no part in this thesis submitted elsewhere as a part of an any other or the same degree program.

.....

Date

.....

J.M.R Jayasinghe

I endorse the declaration by the candidate.

.....

Mr. A. M. P. B. Samarasekara.

Supervisor.

Date: .....

.....

Dr. D.A.S. Amarasinghe

Supervisor.

Date: .....

## Abstract

Cotton is a natural staple fiber that almost consist with cellulose compared to wood. The major economic value of the cotton is in Textile Industry. In the past recent years, cotton consumption demand was increased than the production. In textile industry cotton are blending with various other synthetic fibers such as polyester, nylon and lycra to obtained desirable properties. Therefore, the fabric recycling methods are quite complicated although it is highly available as pre-consumer garment waste. In this work a method was developed to identify the amount of cotton present in the cotton/polyester blended fabric by using Fourier transformed infrared (FTIR) second-order derivative spectrum. Then the cotton waste composition was determined and used to extract cellulose. Then purify cellulose was subjected to extract Micro Fibrillated Cellulose (MFC) by using acid hydrolysis method. MFC has very high economic value compared to cotton fabric waste in various applications such as bio-composites, medicine, cosmetic, pharmaceutical, tissue engineering, bio-sensors, paints and coating, flexible electronics, air filters and high tech applications including aviation and automobile.

However, the major challenge of extracting MFC is the low amount of yield in acid hydrolysis, although it considered to be as most cost effective method of MFC extraction. Laboratory extracted small quantities are not sufficient in industrial applications such as in reinforcing composites. Three experimental factors including; acid concentration, hydrolysis time and temperature show the highest effect in yield and quality of MFC. Therefor this experiment was designed to optimize the three independent factors effect on two responses of yield (%) and Width (nm) of MFC. Response surface methodology was employed to design the experiment and ANOVA statistical test results were used to determine the significance of the parameter effect on acid hydrolysis. Further extracted MFCs physical and structural properties were discussed. Morphological features and size of the fibers were examined by scanning electron microscopy (SEM), structural features and chemical functionality was determined by Fourier transformed infrared (FTIR) spectroscopy, degree of crystallinity was obtained by X-ray diffraction (XRD) spectroscopy and thermal properties were determined by Thermo gravimetric analysis (TGA).

**Keywords:** Micro Fibrillated Cellulose, chemical purification, acid-hydrolysis, second-order derivative spectroscopic method.

## **Acknowledgement**

My foremost gratitude is expressed to my research supervisors Mr. A. M. P. B. Samarasekara and Dr. D.A.S. Amarasinghe for their continuous valuable guidance and great support given to me throughout this research period.

I express my sincere gratitude for all staff members of the Materials Science & Engineering department of University of Moratuwa for their kind assistance and willingness to help for success the research.

Finally, I would like to thankful all of my friends and colleagues who are not been mentioned here personally in making this work success. And specially thanks to my loving parents and brother for their patience, assistance, care and love in all the time.

## Table of Content

Declaration.....	i
Abstract.....	ii
Acknowledgement .....	iii
1. Introduction.....	1
2. Literature Review.....	5
2.1. Cellulose Structure.....	5
2.2. Cotton.....	7
2.3. Cotton fabric recycling.....	8
2.4. Ageing of textiles during laundering .....	8
2.5. Extraction and Classification of Micro and Nanoscale cellulose.....	9
2.6. Optimization of extraction of nanocellulose by acid hydrolysis process.....	11
3. Methodology .....	13
3.1. Cotton fabric characterization.....	13
3.2. Moisture content of the cotton fabric.....	13
3.3. Ash content of the cotton fabric.....	13
3.4. FTIR analysis of cotton fabric and cotton linters.....	13
3.5. XRD analysis of cotton fabric and cotton linters .....	13
3.6. TGA analysis of cotton fabric and cotton linters .....	14
3.7. Composition analysis of cotton-polyester blend.....	14
3.8. Mixture Ratio Analysis by Beer-Lambert law .....	15
3.9. Chemical pre-treatment of cotton .....	16
3.10. Preparation of MCC.....	16
3.11. Design of experiment to optimize the acid hydrolysis parameters .....	17
3.12. Preparation of Microfibrillated-cellulose.....	18
4. Results and discussion .....	22
4.1. Analysis of the polyester amount in cotton/polyester fibre blend.....	22
4.2. Waste cotton fabric characterization.....	30
4.2.1. Moisture content of the waste cotton fabric.....	30
4.2.2. Ash content of the waste cotton fabric.....	30
4.3. Waste cotton fabric and raw cotton linters – FTIR analysis .....	31
4.4. XRD analysis of waste cotton fabric and cotton linters .....	32
4.5. TGA analysis of waste cotton fabric and cotton linters .....	33
4.6. Experimental design to optimized the acid hydrolysis parameters.....	34
4.7. Development of the regression model .....	34
4.8. ANOVA analysis and lack-of-fit .....	35

4.9.	Process Variables Optimization .....	39
4.10.	Contour Plots and surface plot of width of MFC.....	40
4.11.	Contour plots and surface plot of Yield of MFC .....	43
4.12.	FTIR Characterization of the MFC.....	47
4.13.	Morphology of the MFC.....	50
4.14.	Crystallinity of MFC.....	55
4.15.	Thermal degradation behaviour of MFC .....	58
5.	Conclusion .....	59
6.	References.....	61

## List of Figures.

Figure 1 : Classification of cellulose [67]	10
Figure 2: Preparation of MCC from cotton fabric	17
Figure 3: Preparation of MFC by using MCC as the starting material	20
Figure 4: Acid hydrolysis slurry of cellulose	20
Figure 5: Final freeze dried sample	21
Figure 6: Characteristic absorption spectrums of cotton/polyester blended samples	22
Figure 7: The FTIR spectrum of 100% cotton and the 100% polyester	25
Figure 8: The FTIR first-order derivative spectrum wavenumber range of 1573 - 1860 $\text{cm}^{-1}$ .	26
Figure 9: The FTIR second order derivative spectrum wavenumber range of 1573 - 1860 $\text{cm}^{-1}$	26
Figure 10: Absorption versus amount of polyester present in fiber blend	29
Figure 11: Absorption versus amount of polyester present in fiber blend	29
Figure 12: FTIR spectra of celluloses present in the cotton linters and the cotton fabric	31
Figure 13: X-ray diffraction patterns of raw cotton linters and cotton fabric	32
Figure 14: TGA curve for cotton linters and the waste cotton fabric	33
Figure 15: Parato chart of standardized effect of concentration, time and temperature on width of MFCs	37
Figure 16: Pareto chart of standardized effect of concentration, time and temperature on yield of MFCs (response is yield (%), $\alpha = 0.05$ )	39
Figure 17: Surface plot of mean width vs. time and concentration (hold temperature)	40
Figure 18: Contour plot of mean width vs. time and concentration (hold temperature)	40
Figure 19: Surface plot of mean width vs. temperature and concentration (Hold time)	42
Figure 20: Contour plot of mean width vs. temperature and concentration (hold time)	42
Figure 21: Surface plot of yield vs. time and concentration (hold temperature)	43
Figure 22: Contour plot of yield vs. time and concentration (hold temperature)	43
Figure 23: Surface plot of yield vs. time and concentration (hold time)	45
Figure 24: Contour plot of yield vs. time and concentration (hold time)	45
Figure 25: FTIR Spectrum of MFC samples	48
Figure 26: FTIR spectra of celluloses studied in the region between 1512 $\text{cm}^{-1}$ to 800 $\text{cm}^{-1}$	49
Figure 27: Cellulose fibres of sample MFC 8	50
Figure 28: Cellulose fibers of sample MFC-09	51
Figure 29: Cellulose fibres of sample MFC 2	52
Figure 30: Cellulose fibers of sample MFC 14	53
Figure 31: XRD patterns of MFC	56
Figure 32: TGA curves of MFC	58



## List of Tables

<i>Table 1: Cotton Polyester blend weights and identification.</i>	14
<i>Table 2: Parameter levels of experiment</i>	18
<i>Table 3: Experimental coded values and results of Mean width and Yield</i>	19
<i>Table 4: Identification of cotton polyester FTIR Wave number values [70]</i>	23
<i>Table 5: Summary of the FTIR spectroscopic data for polyester in each series.</i>	28
<i>Table 6: The moisture content of the waste cotton fabric</i>	30
<i>Table 7: The Ash content of the waste cotton fabric</i>	30
<i>Table 8: Independent variable used for the experiment and their coded values</i>	35
<i>Table 9: ANOVA statistical analysis and the lack-of-fit test results for width of the MFC</i>	36
<i>Table 10: Modal summary</i>	36
<i>Table 11: the ANOVA statistical analysis and the lack-of-fit test results percentage yield of the MFC.</i>	38
<i>Table 12: Model summary</i>	38
<i>Table 13: Microfibrilated cellulose samples that gives minimum values for the width.</i>	46
<i>Table 14: The crystal structure given band position in <math>2\theta^\circ</math> and their d-spacing values.</i>	57

## 1. Introduction

Micro/nanocellulose gained the attention of scientist due to their unique characteristics that have led to applications of great potential. Micro/nano scale cellulose is described as a type of native cellulose that is existent in many plants and bacteria. These native Micro/nanocellulose can be divided into four main types. They are; Nanocrystalline cellulose (NCC) or nano whiskers, Nanofibrillated cellulose (NFC), Micro fibrillated cellulose (MFC) and Bacterial Cellulose (BC) [1].

Cellulose is considered the most abundant natural polymer carbohydrate that can be found everywhere in the world and is biodegradable in nature. Nanocellulose shows dominant physical properties including; high specific strength, high surface area and specific surface chemistry. It also exhibits biological properties such as biodegradability and low toxicity, renewability and low CO<sub>2</sub> emissions into the atmosphere during their production cycle [1-5]. In recent years researchers have significantly mentioned Micro/nano scale cellulose in a variety of potential applications, specifically in bio-composites, medicine, cosmetic and pharmaceutical applications, tissue engineering, bio-sensors, paints, and coating as well as flexible electronics, air filters and high tech applications such as aviation and automobile [6-8].

Numerous methods have been used in literature for the purpose of characterization and classification of Micro/nano scale cellulose. Transmission Electron Microscope (TEM), Field Emission Scanning Electron Microscope (FE-SEM) and Atomic Force Microscope (AFM) were used to identify the width and the length. X-ray Diffraction Spectroscopy (XRD) was utilized to identify the crystalline structure and the degree of the crystallinity. Fourier Transformation Infrared (FTIR) spectroscopy was used to identify the chemical functionality of the cellulose and indirectly used to calculate the crystallinity index of the nanocellulose. Thermal degradation behavior was studied through the data obtained from Thermal Gravimetric Analysis (TGA). Solid State Nuclear Magnetic Resonance (ssNMR) was performed to analyse the presence of anisotropic interactions of crystalline cellulose. The surface charge of the stable colloidal suspension was measured by conductometric titration [7-15].

Throughout history many sources were utilized to isolate the cellulose fibres and nano scale cellulose including; wood, hemp, jute, banana fibres, pineapple leaves, coconut palm petiole, rice husk, wheat straw, bacteria, algae and tunicate. Bacterial cellulose is considered as purest form of the cellulose since it does not contain hemicellulose and lignin. When comparing with the sources of plants, the highest purity and yield was reported by cotton linters, since cotton consists 95% of cellulose [15-22].

When Micro/nano scale cellulose was introduced into the polymer matrix, significant properties were observed. It possessed the ability of acting as a reinforcing filler material to enhance the strength, impact resistance and hardness of the composite. Physical properties of the NFC was previously reported as the young's modulus along the axis gives a value of 167.5 GPa. The experimental analysis of elastic modulus of nanowhiskers was 143 GPa [20, 22, 25] while the larger surface area about 150 m<sup>2</sup>/g and high aspect ratio of 1:70 are again significant [23]. These outstanding physical properties enhance the overall properties of the composite and lead to bio-degradation at the end of the life cycle of the product.

NFC/MFC and NCC nano structures are produced destructively by converting large size units (mm) in to smaller units (nm). Cellulose extraction was first reported in 1932 by Eisenhut and Schlartz [26,27]. After the 1980s, different methods were reported to isolate nanocellulose namely; acid hydrolysis with chemical pre-treatments, enzymatic treatments and mechanical treatments such as cryocrushing, Ultrafine grinding, electrospinning method and ultrasonic technique. The degree of crystallinity and the amount of amorphous domain of the native cellulose varies with the source of the cellulose. Therefore, the extracted cellulose properties are highly dependent upon the source of the cellulose [27-32].

The major economic value of cotton is in textile production while minor amounts are used in paper industry, crafts and filters. Cotton fabric can be used to extract cellulose with less number of chemical purification steps. Cotton recycling and reusing were rarely reported throughout the history and a few articles were found when reviewing literature. Cotton material recycling can be categorized into two types, pre-consumer cotton waste recycling and post-consumer cotton waste recycling. Pre-consumer cotton waste is usually generated by the waste of excess yarn or cut fabrics

while post-consumer cotton is generated at the end of the life cycle of a cloth. These two types of cotton have very different properties, because post-consumer cotton undergoes ageing conditions after laundering and drying [34,35]. In recent years, recycled cotton has been used with recycled plastic bottles to produce sustainable environmentally friendly products like polishing and wiping cloths, high-quality papers, etc. The main obstruction which discourages cotton recycling is the fibre blending with many other synthetic polymers like polyester, nylon and lycra. Although cotton can be comfortably used to extract cellulose, commercially available cotton materials are usually blended with polyester [36].

When compared with wood and non-wood materials, cotton fabric can be used to extract cellulose with minimal chemical processing. Therefore, the key objective of this study is the extraction of microfibrillated cellulose by using recycled cotton waste. Cotton textile waste recycling and conversion to MFC can be considered a notable economic value addition. Commercially available white textile cotton waste of 10kg would be approximately priced at about 2 USD. According to the Nanografi Nano Technologies and Cellulose Lab Industries in 2020, the best price of 10gs of MFC/NFC is 13.5 USD [37]. Since cotton fabrics are usually blended with polyester, the secondary objective of this study is to develop a simplified method to identify the purity of cotton waste. FTIR derivative spectroscopic method was developed to determine the composition of the waste fabric since FTIR is frequently use in the polymer and textile laboratory in Sri Lanka. The major challenge of extracting MFC is their low amount of yield in acid hydrolysis, although it is considered to be the most cost-effective method in MFC extraction. The small quantities extracted by laboratories are not sufficient for industrial application such as reinforcing composites, improving rheological properties and the biodegradability of plastic [28,31,33]. Therefore, optimizing the major parameters of the acid hydrolysis process by using Response surface methodology is a secondary objective of this work. The three most critical parameters which are sulfuric acid concentration, hydrolysis time and temperature were optimized in hydrolysis reaction. The mean size of the width of the cellulose fibres  $Y_{\text{size(nm)}}$  and the yield  $Y_{\text{yield(\%)}}$  was measured as the response.

Box-Behnken design was used to obtain the response surface to illustrate the effect of the significant factors of acid hydrolysis. Both independent variables of  $Y_{\text{yield}(\%)}$  and  $Y_{\text{size}(\text{nm})}$  subjected to ANOVA statistical test to identify the significant effect of each parameter. Based on the statistical data obtained, the most optimized hypothesis was given for the sulfuric acid concentration, hydrolysis temperature and hydrolysis time. The resultant microfibrillated cellulose were taken for further instrumental analysis for a detailed study. Morphological features and size of the fibres were examined by scanning electron microscopy (SEM), structural features and chemical functionality was determined by Fourier transformed infrared (FTIR) spectroscopy. The degree of crystallinity was obtained by X-ray diffraction (XRD) spectroscopy and thermal properties were determined by Thermo gravimetric analysis (TGA).

## 2. Literature Review

### 2.1. Cellulose Structure

The structure of cellulose first reported in 1838, was discovered as a type of sugar in a green plant cell wall by a chemist called Anselme Payen. There are many natural polymer fibres can be found in nature such as proteins like silk and wool and carbohydrates like cellulose in cotton [1-2]. Cellulose is a highly abundant natural polymer in nature that has a unique organic structure. Cellulose form thin fibres called micro fibrillated cellulose that have a very high aspect ratio. They construct highly interconnected three-dimensional network in the lignin matrix. Usually cellulose is associated with hemi-cellulose, pectin and lignin. In wood cellulose form, strong cell walls together with the lignin matrix are referred to as a biopolymer composite [6]. Cellulose can also be found in some bacteria and cotton that are not tightly bound with the lignin matrix. In cotton, cellulose exists as a thin, hollow hair-type fibre wrapped around cotton seeds. When cotton seeds mature, these tiny hair-like structures become elongated and the airborne dispersion of seeds in dry air [6-9].

Cellulose is a polysaccharide that consists of  $\beta$ -D-glucose units linked by  $\beta$  (1 $\rightarrow$ 4)-glucosidic bonds. This organic compound has  $(C_6H_{10}O_5)_n$  formula where n may be varying from a long range of thousands of  $\beta$  (1 $\rightarrow$ 4)-glucosidic bonded glucose units. The degree of polymerization (DP) can be represented by the number of linked glucose units and varies with the type of cellulose source. As for the cotton, the degree of polymerization was about 15000 [5-7].

Cellulose form highly leaner and long chain of molecules, which make due to that cellulose insoluble in water. In cellulose fibres, about 100-300 of cellulose chains are grouped and bonded by hydrogen and van der Waals bonds. Each monomer consists of free three hydroxyl group from chain ring [5]. These hydroxyl groups make the inter and intra molecular hydrogen bonds, and these hydrogen bonds determine most of the physical properties of the cellulose. The intra-chain hydrogen bonds that are formed within the same polymeric chain responsible for the straightness and the stability of the cellulose chain. The hydrogen bond that was created by the hydroxyl groups and the

van der Waals forces determine the structure and the crystallinity of the cellulose [5-8]. Inter chain hydrogen bonds that are formed in-between the monomers and van der Waals forces collect and bond the neighbouring cellulose chains together and form the microfibrils in plant cells. This inter and intra chain hydrogen bonds and van der Waals forces determine the three-dimensional network of the cellulose and creates a stable polymer. This also determines the crystal structure of the cellulose and the degree of crystallinity. The highly-ordered structure of the cellulose leads to higher degree of crystallinity and thereby provides the stiffness to the cellulose matrix [5,7,9,10].

Cellulose is available as several different types including Cellulose I, II, III and V of polymorphous in accordance to their crystal forms. Cellulose I is considered to be the native cellulose that has two crystalline forms called cellulose I $\alpha$  and I $\beta$ . Wherein, cellulose I $\alpha$  has triclinic unit cell formed by one single chain. The cellulose I $\beta$  is created by a monoclinic unit cell using two adjacent polymer chains [5-7]. These polymorphous can be interchanged by utilizing heat and chemical recreation. Cellulose I is referred to as the most abundant type of cellulose in nature and has less thermodynamically stable. Cellulose I is less stable than cellulose II in nature, therefore Cellulose I is termed as meta stable [7-13].

The difference between cellulose I and II is their difference between the stability which is determined by the direction of the chains. In native cellulose or cellulose I, the polymer chain is aligned in parallel while the stability of the cellulose of cellulose II is determined by their non-parallel chain alignment. However, the structure of cellulose is highly complicated due to their number of hydrogen bonding arrangement. The inter and intra hydrogen bonding of the cellulose chain provides the rigidity and stiffness to cellulose as a material. Due to their crystal structure arrangement cellulose form the ring sheets in their origin. These sheets of cellulose in the cellulose microfibrils that was smallest element of cellulose fibres. These fibres then fibrillate with each other forming long cellulose fibres in the plant cell wall and are immersed in the lignin matrix. Therefore, the nanocellulose is created by destructively breaking down the structure of cellulose long fibres and removing their amorphous part [14,16,18].

## 2.2. Cotton

Cotton is a natural resource that consists of cellulose and is considered to be the purest form of the naturally occurring cellulose apart from bacterial cellulose. Cotton fibres are the hair of its seeds that we use in the textile industry. This hair-like structure around the cotton seed helps it to disperse with dry air. The matured cotton hair is a hollow fibre and considered as a single cell built by cellulose with small traces of hemicellulose pectin and waxes. Therefore, with a minimal chemical purification process, we are able to isolate cellulose from cotton than the upper plant cells. It can be considered that 99% pure cellulose can be obtained by the matured, healthy cotton [22].

Cotton fibres are removed with ease from matured cotton seeds. These fibres are thin and lengthy while some tiny fibres remain with the seeds. These tiny fibres are usually referred to as cotton linters in the textile industry. The matured lengthy fibres that are used to produce textile apparel are called lint. Moreover, these linters are used in other low economical applications such as papers, filter papers and as a cotton source [33]. These two types of cotton fibres should have two different properties but have not been studied in-depth yet. Cotton linters are considered to be the purest form of cellulose and most researchers use it for experimental purposes. According to current literature, cotton linters were used in many researches to extract Nano-cellulose due to its purity [33,34,35].

Cotton is cultivated in tropical countries as an economic crop on a large industrial scale due to their high demand in the textile industry. Africa, Pakistan, India, China are major cotton producers according to the World Agricultural Organization. The figures of world cotton demand and production provided by the USDA, World Agriculture Supply and Demand Estimates Report shows that after the year 2015, the consumption and demand for cotton had exceeded the capacity for the production of cotton. Therefore, recycling methods to re-use cotton can be a crucial way of circumventing this gap between demand and supply [25, 27]. Unfortunately, the World Food and Agricultural organization reported that the 95% of post consumable cotton is unutilized, ending up in landfills. Landfilling and burning cotton waste releases a considerable amount of greenhouse gasses in to the environment while also emitting a foul odor



when decomposing under anaerobic conditions. On the other hand, the post recycling cotton was demotivated due to fabric blending. To obtain the desired textile properties, the cotton fibres are usually blended with synthetic fibre yarns like polyester and nylon. Therefore, the separation of this synthetic part of the cotton blend is another potential research area in cotton recycling [36].

### **2.3. Cotton fabric recycling**

Cotton fabric recycling has still not gained sufficient attention in the textile industry. Although, some research has been developed to separate cotton from the textile blends and reuse the cotton fibres. There are very few articles in relation to the recycling and reuse of cotton textile. Some biological and chemical routings have been developed to facilitate cotton recycling. Cotton that is used in recycling can be categorized in to pre-consumer and post-consumer cotton waste. Pre-consumer cotton waste is generated usually by the waste of excess yarn or cut fabrics while the post-consumer cotton is generated at the end of the lifecycle of clothes. These two types of cotton have different properties because post-consumer cotton will have undergone aging conditions after laundering and aging [33, 34]. In recent years, recycled cotton has been utilized in several applications. One example is combining it with recycled plastic bottles to create new textiles that can be used to produce sustainable and environmental-friendly products such as a polishing and wiping cloths, high quality papers etc [34]. The major reason for discouraging cotton recycling is due to the blending of cotton fibres with many synthetic polymers such as polyester, nylon and lycra. Therefore, this area is currently under research, review and development while insufficient attention has been given to the extraction of cellulose from cotton fabric waste [16, 17, 18].

### **2.4. Ageing of textiles during laundering**

In the post cotton recycling process, it is necessary to understand the aging of cellulose in the fabric laundering and drying process. During laundering, cellulose fibres lose their physical properties and become more brittle while also losing their degree of polymerization. When chemically purifying the cotton, it removes hemicellulose usually associated with cellulose and some amount of pectin and other

polysaccharide impurities with a small amount of waxes. Due to the removal of these elements, fibres become more swellable after chemical purification. During the laundering process, this swellable nature of cellulose is lost and this is referred as hornification. This phenomenon cannot be reversible once established [33, 34].

Laundering with detergent and drying under direct sunlight introduced harsh conditions to the textile fibres. This conditions alter and degrade the structure of cellulose in their molecular level. Therefore, after laundering the original physical properties of the cotton fibres will be clearly lost due to the reduction of the degree of polymerization. This ultimately reduces the mechanical strength of the fibres. The alkaline environment induced by the usage of detergent during laundering, causes the peeling of cellulose which is also referred to as a peeling reaction. This results in the continuing degradation at the end of the polymer chain. Therefore, the post-consumer cotton waste cannot be used as a native cellulose source to extract good quality cellulose [33].

## **2.5. Extraction and Classification of Micro and Nanoscale cellulose**

Nanocrystalline cellulose was produced using acid hydrolysis with Hydrochloric acid (HCl), Sulfuric acid (H<sub>2</sub>SO<sub>4</sub>), Phosphoric acid (H<sub>3</sub>PO<sub>4</sub>) with or without the presence of a catalyst. Nanocrystalline cellulose isolation was first reported in 1959 and referred to as “micelles”. Subsequently, it was referred to as nanocrystalline cellulose or nano whiskers. Historically, many sources have been used to isolate nanocrystalline cellulose, including: wood, cotton, hemp, jute, sugar cane, wheat straw, algae, tunicate etc but most researchers use cotton linters instead [8, 9, 11]. The yield of cellulose and the quality of cellulose depend on the source of native cellulose, isolation method, acid concentration and time. The yield of the Nano crystalline cellulose varies from the 20% to 70% according to the source of cellulose. Generally, the maximum yield was reported around 30% [12,15]. The crystallinity of the nanocellulose and thermal properties are widely studied areas in scientific literature. The thermal degradation of cellulose start at 315 °C in comparison to crystalline cellulose which begins at 360°C [7, 13].

The application of nanocrystalline cellulose is wide and includes; Biomedical applications, pharmaceutical and cosmetic as well as in bio-composite applications. These nano scaled elements can be introduced in to the polymer matrix and usually possess outstanding physical and mechanical properties. Most notably, its ability of reinforcement, which is remarkable. The Young's modulus of native cellulose along the axis gives a value of 167.5 GPa. The experimental analysis of elastic modulus of nanowhiskers is 143 GPa (Mathew and Kristiina, 2006). Larger surface area of about 150 m<sup>2</sup>/g and high aspect ratio of 70 are also significant in nanocellulose (Tang and Yang, 2014).

Microfibrillated cellulose properties are less studied compared to nanocrystalline cellulose. MFC is secured by the fibrillation nature of cellulose fibres. By chemical pretreatment or mechanical shearing the cellulose fibres were expanded in to the three-dimensional network that leads to a larger surface area. Cellulose fibrils diameter in MFC were very thin and obtained at nanometer level while the length lay in several microns.

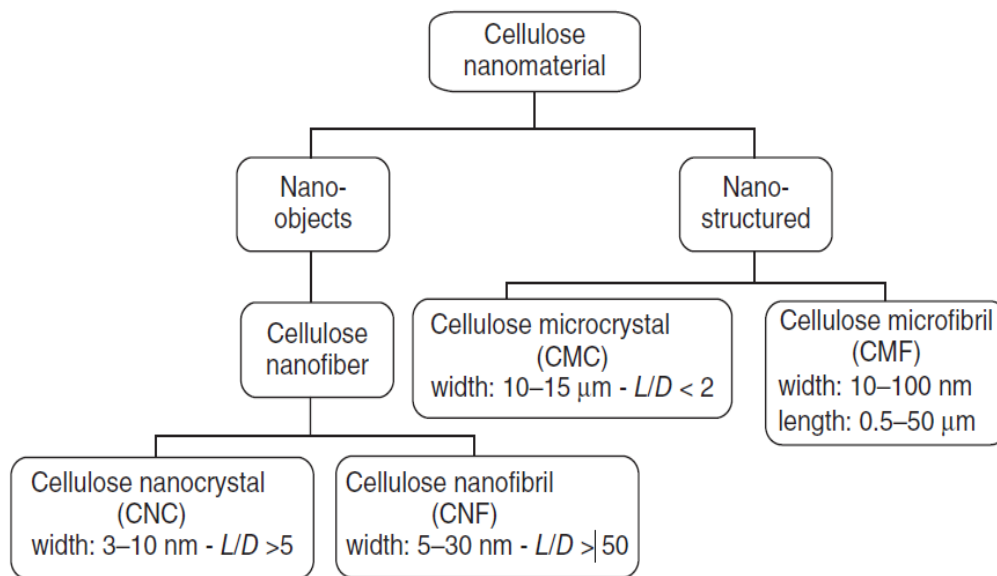


Figure 1 : Classification of cellulose [67]

MFC differs from native cellulose due to its larger surface area. MFC powder has the ability of holding a high amount of water and to form gel even at low concentrations due to a large number of surface hydroxyl groups. The aspect ratio of the MFC was very high and leads to high strength in reinforcing composites, barriers and thin films. The fundamental reason for using MFC is its strengthening ability and low weight. It can reduce the weight of the material and simultaneously enhance the strength significantly. It was reported that 1% of MFC can result in 18%-20% product performance enhancement. MFC fibres are strong as carbon fibres and stiffer than the glass fibres and lighter in weight [23,25,32].

## **2.6. Optimization of extraction of nanocellulose by acid hydrolysis process**

Response surface methodology is a mathematical and statistical tool that is used to optimize the chemical process. Improving the performance of the process by optimizing process parameters without increasing the cost is important in the industry. The level of parameter changes to determine the optimal experimental condition while keeping the other factors constant. This is referred to as the one-variable-at-a-time practice. This practice has some advantages as it does not demonstrate interactive effects among the variables and total effects of the individual parameters on the optimizing process. Response surface methodology is a collaboration of mathematical and statistical practices that can be used for developing, improving and optimizing processes when several factors influence simultaneously in one process. Therefore, this method is highly used in new product formulation developments and improving existing product developments in Engineering [56-58].

Foremost in Response surface methodology is to design the experiment abbreviated as DoE – Design of experiment. The main objective of DoE is the selection of the independent variables and points that are needed to evaluate the response [56, 58, 60]. The chemical process includes many parameters that significantly influence the quality and yield of the product. So, it is necessary to identify the significant parameter(s) that have a major effect on process outcome. Pre-screening experiments or a preliminary analysis was useful in the correct identification of the independent experimental parameters.

Cellulose extraction by acid hydrolysis is a widely researched area since the 1930s. Many publications were found on the reactive conditions of acid hydrolysis in NCC extraction. There are very few studies on the effect of individual reactive factors and their correlation to each factor. Reviewing the literature, two experiments were found on acid hydrolysis process optimization for extract nanocellulose [56-61].

Optimization of Nanocrystalline cellulose extraction from Microcrystalline cellulose was first reported in 2006 by Daniel Bondeson and Aji Mathew. Their primary objective was to obtain a rapid yield of nano-cellulose by optimizing the parameters of acid hydrolysis of MCC. They selected four factors and two responses. Four variables including Sulfuric acid concentration, hydrolysis time, temperature, initial MCC concentrating and ultrasonication time effect were studied and fitted into a  $3^4$  factorial design. Each variable consisted of three levels of variation. The study concludes that sulfuric acid concentration and hydrolysis time have an apparent interaction. The results show that a sulfuric acid concentration of 63.5% (w/w), can produce cellulose Nano whiskers with a length between 200-400 nm and a width less than 10 nm with approximately two hours of reaction time and 45 °C temperature. In NCC extraction acid concentration, solid/liquid ratio, reaction temperature and reaction time are significantly affected in the total NCC yield [64].

A further study as reported in 2010, was the optimization of acid hydrolysis parameters in the extraction of nanocrystalline cellulose from cotton linters by Chih-Ping Chang and Chen Wang.  $2^4$  factorial design for the effect of acid concentration, temperature, hydrolysis time and solid liquid ratio on the yield of the nanocrystalline cellulose were studied. The influence of the four factors shown was significant when the acid concentration and solid/liquid ratio approached a higher level, or the reaction temperature and reaction time shifted to the lower level. It was observed that the best NCC yield was given by the acid concentration of 60%, a solid/liquid ratio of 1:20, reaction temperature of 45°C and reaction time of five minutes [65].

### **3. Methodology**

#### **3.1. Cotton fabric characterization**

Waste cotton fabric pieces were used as an initial native cellulose source. Commercially available fabrics are usually blended with polyester yarns to obtain the desired qualities in textile. Therefore, a method was developed to identify the amount of polyester that is present in cotton/polyester blended fabric. Then, the purity of cotton fabric was examined. Cotton fabric's moisture content, ash content, FTIR spectroscopy, XRD spectroscopy and TGA curve was obtained and results were discussed.

#### **3.2. Moisture content of the cotton fabric**

Five cotton fabric samples (about 10g) were kept at 105 °C until a constant weight in a furnace was achieved. The weight of the residue samples was then measured.

#### **3.3. Ash content of the cotton fabric.**

Five cotton fabric samples (about 8g) were burned at 500 °C for five hours in a furnace. After combustion, the ash residue weight from each sample was measured.

#### **3.4. FTIR analysis of cotton fabric and cotton linters**

Cotton contained a relatively very high amount of cellulose. Apart from this, hemicellulose, Pectin, Lignin and waxes were present in trace amounts as a mixture of hydrocarbons, alcohols, esters and free acids that have long polymer chains. The chemical functionality of the raw cotton fabric and raw cotton linters were determined in transmittance mode of ATR-FTIR. All spectra were observed by the accumulation of 64 scans, with a resolution of 2 cm<sup>-1</sup> at 650–3600 cm<sup>-1</sup> and were then compared.

#### **3.5. XRD analysis of cotton fabric and cotton linters**

Cellulose can be found in nature as various types including Cellulose I, II, III, and V. Cellulose I is considered as a native cellulose type in nature, while Cellulose II are chemically regenerated cellulose usually made in laboratories. Each type of cellulose has their own characteristics and well defined XRD patterns that correspond to the crystalline domain of cellulose molecules. Cellulose I carries a significant amount of crystalline domain that has two crystal structures I $\alpha$  and cellulose I $\beta$ . Therefore, XRD analysis was carried out to identify the content of cellulose I in the cotton fabric as well

as confirm the degree of crystallinity. XRD analysis of the cotton linters and cotton fabric was determined with a diffractometer CuK $\alpha$  radiation. X-ray diffractograms were obtained at room temperature within a  $2\theta$  ranging from  $5^\circ$  to  $40^\circ$  with a scan rate of  $2^\circ\text{min}^{-1}$ . The crystallinity index (Icr) of the cotton linters and the cotton fabric was identified.

### 3.6. TGA analysis of cotton fabric and cotton linters

The dehydration and the thermal degradation behaviour of the cotton fabric and the linters were characterized through thermogravimetric analysis (TGA). A specimen of 15 mg was tested under a nitrogen environment at a temperature range  $25\text{ C}^\circ$  to  $400\text{ C}^\circ$ . The heating rate temperature was  $5\text{ C}^\circ\text{min}^{-1}$ .

### 3.7. Composition analysis of cotton-polyester blend

Derivative FTIR spectroscopic method was developed to identify the amount of polyester present in the cotton/polyester blend. The quality of cellulose present in the fabric finally affects the quality of extracted cellulose. Properties present in cotton may decrease during the chemical treatment of the fabric mainly during the bleaching, laundering and dyeing of yarns. FTIR spectroscopy provides information about the composition of the ingredients present in the product. FTIR absorption spectrum provides quantitative information of the composition of the sample. To obtain the blend of cotton and polyester, raw cotton linters and commercially available 100% polyester yarn (Fiber-line international, Netherlands) were used. Weighted amounts of cotton/polyester mixed fibre samples were prepared as per the below-mentioned weight given in table no 1. They were mixed together by pre-determined ratios and bleached under vigorous and constant mechanical stirring with 35%(w/w)  $\text{H}_2\text{O}_2$  until a uniform stain-free white fibre mix was obtained.

Table 1: Cotton Polyester blend weights and identification.

Sample no	CP1	CP2	CP3	CP4	CP5	CP6	CP7	CP8	CP9	CP10	CP11
Cotton:polyester weight (g)	10:0	9:1	8:2	7:3	6:4	5:5	4:6	3:7	2:8	9:1	0:10

The mix of fibres finally obtained were dried at room temperature and subjected to FTIR analysis. The model was developed by absorption peak intensity changing with the change of polyester composition at the particular wavenumber range.

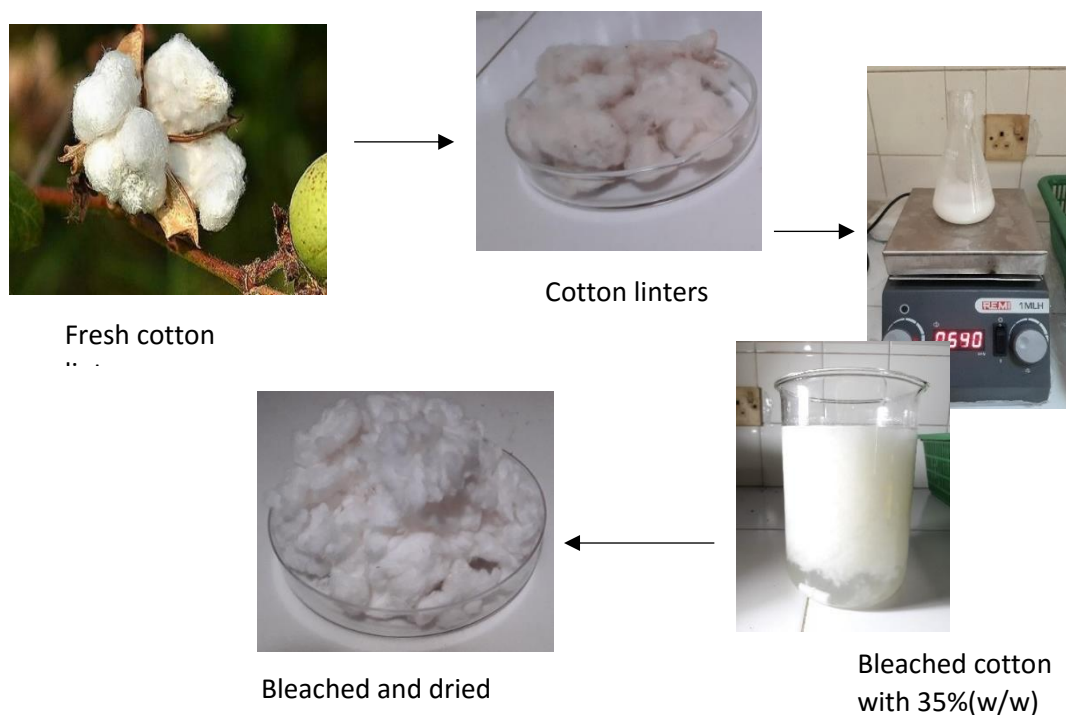


Figure 1: Preparation of bleached cotton from cotton linters

### 3.8. Mixture Ratio Analysis by Beer-Lambert law

Amount of cotton content present in blended fabric can be determined by the FTIR derivative spectroscopy. All the ATR-FTIR spectra were taken in Absorption mode with a resolution of  $2\text{ cm}^{-1}$  at  $500\text{--}4000\text{ cm}^{-1}$ . Quantitative data was obtained using the second order derivative spectroscopic peak height ( $D_L$ ) that was given at the wave number range of  $1740\text{--}1713\text{ cm}^{-1}$ . The absorption spectral band of polyester gives the maximum intensity peak for the characteristic C=O str bond which appears at  $1740\text{ cm}^{-1}$ . This intensity of the peak depends upon the particular polyester chemical structure of substances and can be used to quantify the amount of polyester present in the particular sample. The derivative spectroscopic technique is a useful method that



can be used to identify the hidden bands of the broad spectrum. The obtained results of 1<sup>st</sup> and 2<sup>nd</sup> order derivative spectroscopy data were then validated and compared with linearity and precision. Afterwards, obtained  $D_L$  values were applied to Beer-Lambert law.

### **3.9. Chemical pre-treatment of cotton**

Selected pure cotton fabric pieces were used as starting native cellulose source. Fabric was soaked in water, cleaned and dried. FTIR analysis was conducted in fabric selection to identify the amount of cellulose present. Cellulose extraction was done after two purification steps – alkali and bleaching treatments. Alkali treatment was carried out to ensure the removal of hemicellulose and other polymeric components and then bleached to remove lignin, dye and stain in fabric. Fabric samples were cut into very small pieces and then bleached using  $H_2O_2$ . 50 g of raw material was mixed with a 1:10 weight ratio of 35%  $H_2O_2$ . Then the solution was heated to 70 °C for two hours, and washed by successive filtration. Alkali treatment was conducted with sodium hydroxide (10% w/w) at 70 °C for two hours, filtered and washed with distilled water until pH = 10 was achieved. Chemically purified and bleached cotton fibres were then dried and subjected to analysis.

### **3.10. Preparation of MCC**

The bleached cotton fibres were hydrolysis using the 35  $H_2SO_4$ % (w/w) with 1:20 solid to liquid ratio. Throughout the reaction, the temperature of the reaction mixture was kept at 40 °C for one hour. During the reaction period mixture was mechanically stirred with a Teflon bar element. After one hour, the reaction was stopped by cooling and diluting the reaction mixture. The obtained residual was washed and filtered until the washed filtrate become neutral. The MCC powder obtained was then oven-dried, measured and stored in cool (18 °C) temperature until further use.

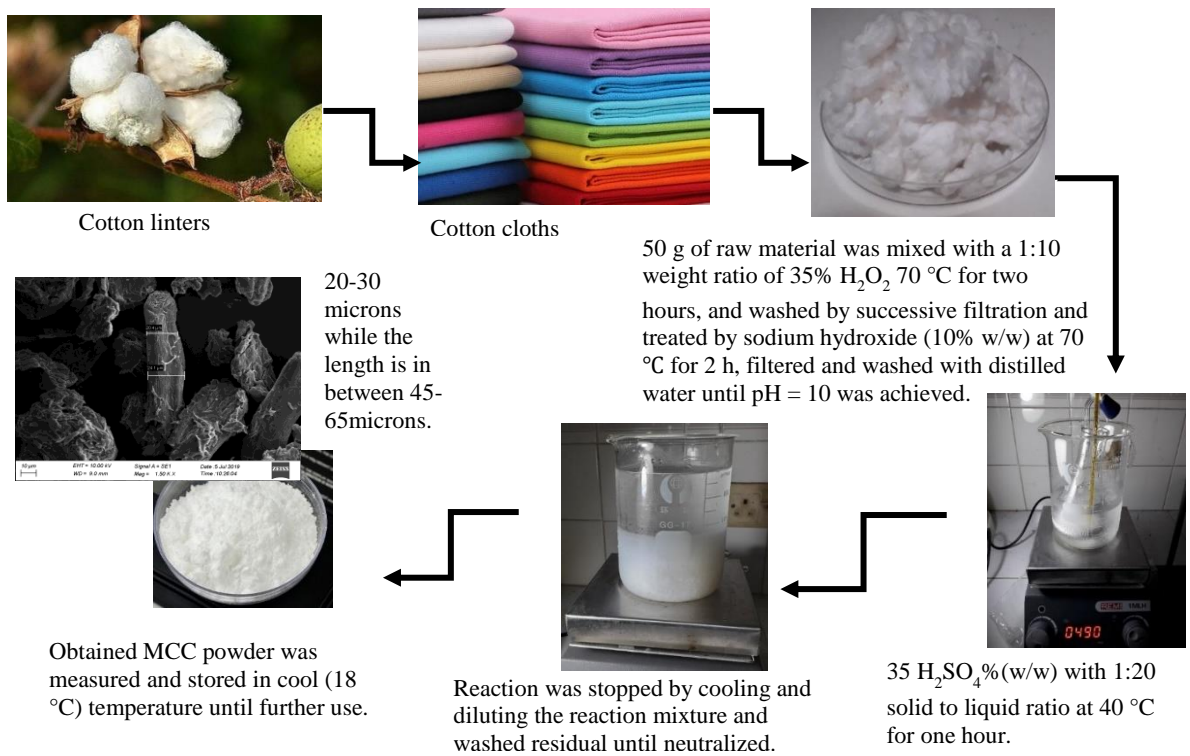


Figure 2: Preparation of MCC from cotton fabric

### 3.11. Design of experiment to optimize the acid hydrolysis parameters

To create the experimental design of Response surface methodology, the Box Behnken experimental method was used as it requires a fewer number of trials in comparison to the Central Composite Design. Three different critical factors were selected, including; H<sub>2</sub>SO<sub>4</sub> Concentration, Hydrolysis time and temperature as well as two responds of mean yield and mean value of fibre width. The variable involves three levels as shown in table no 2. These factor levels are selected according to the previously reported experiments (22).

A comprehensive detailed plan of the levels and the factors are shown in the table below. The lower level of the factor  $x_i = -1$ , Middle level of the factor  $x_i = 0$  and high level of the factor  $x_i = 1$  are represented as follows.

The X is defined as;

$$X = \frac{(x - [x_{max} + x_{min}])/2}{[x_{max} - x_{min}]/2} \dots\dots\dots (2)$$

When selecting the levels, special attention was paid to the range of the level. This was because if the range of the levels were too high, the prediction power of the model would drop down. Therefore, the levels of the experiments were decided only after careful investigation around the literature published about MFC.

Table 2: Parameter levels of experiment

Parameters	Units	Low level $x_i = -1$	Middle level $x_i = 0$	High level $x_i = 1$
<b>X<sub>1</sub> H<sub>2</sub>SO<sub>4</sub> Concentration</b>	w/w	48	52	56
<b>X<sub>2</sub> Hydrolysis time.</b>	min	20	60	100
<b>X<sub>3</sub> Temperature.</b>	°C	40	60	80

### 3.12. Preparation of Microfibrillated-cellulose

Previously prepared MCC was used as the starting material of the MFC. The extracted micro crystalline cellulose from cotton fabric were rod-shaped and in between 80-40  $\mu\text{m}$  in length and 10-20  $\mu\text{m}$  in width in accordance with the SEM observation. 98% concentrated sulfuric acid was used as the hydrolysis agent. Before acid hydrolysis, the extracted MCC was oven-dried and accurately weighted into 5g specimens and then hydrolyzed under different conditions as summarized in Table no 3. Firstly, a water MCC suspension was prepared by adding desired amounts of water to the powder in a conical flask and then placing it in an ice bath while continuously stirring it at 420 rpm to prevent unnecessary heating. Afterwards, the concentrated sulfuric acid was added in drop by drop until the desired amount of acid concentration achieved. The slurry of suspension obtained was then heated while constantly stirring. The reaction was terminated by adding extra amounts of deionized water and the system was then cooled down to 10 °C. The post reacted liquid pulp was then washed by adding distilled water and centrifuge under 10000rpm for 10 minutes and repeated for three cycles. The final washing was followed by conducting a dialysis process until washed water reached a constant pH. After a 72-hour dialysis, the samples were sonicated at 20 – 25 kHz with an output power of 800 W in an ice bath for 10 minutes to avoid the generation of excess heat. The samples were then freeze dried and subjected to analysis.

Table 3: Experimental coded values and results of Mean width and Yield

Sample no	Temperature	Time	Concentration	Mean width (nm)	Yield%
1	0	0	0	440	27
2	1	-1	0	340	20
3	0	1	-1	770	32
4	-1	-1	0	1200	31
5	0	0	0	430	27
6	0	-1	-1	530	23
7	0	-1	1	490	29
8	1	0	1	140	18
9	1	1	0	245	22
10	-1	0	-1	680	30
11	-1	1	0	707	31
12	0	0	0	439	28
13	-1	0	1	1090	24
14	1	-1	-1	470	20
15	0	1	1	1670	22

The design of the experiment was obtained by Minitab 18 Software. The upper, middle and lower parameters were fairly set to increase the predictive power of the model. The response  $Y_{\text{yield}(\%)}$  were obtained by taking the median weight of three replicates. The width  $Y_{\text{size}(\text{nm})}$  of the cellulose fibres were taken by SEM. Both independent variables of  $Y_{\text{yield}(\%)}$  and  $Y_{\text{size}(\text{nm})}$  were subjected to an ANOVA statistical test to identify the significant effects of each parameter.

Based on the statistical data most optimize hypothesis was given to obtain sulfuric acid concentration, hydrolysis temperature and hydrolysis time. Finally, the best four samples were further examined. Morphological features and size of the fibres were examined by scanning using electron microscopy (SEM). The structural features and chemical functionality were determined using Fourier transformed infrared (FTIR) spectroscopy. While the degree of crystallinity were obtained by X-ray diffraction (XRD) spectroscopy and thermal properties were determined by Thermo gravimetric analysis (TGA).

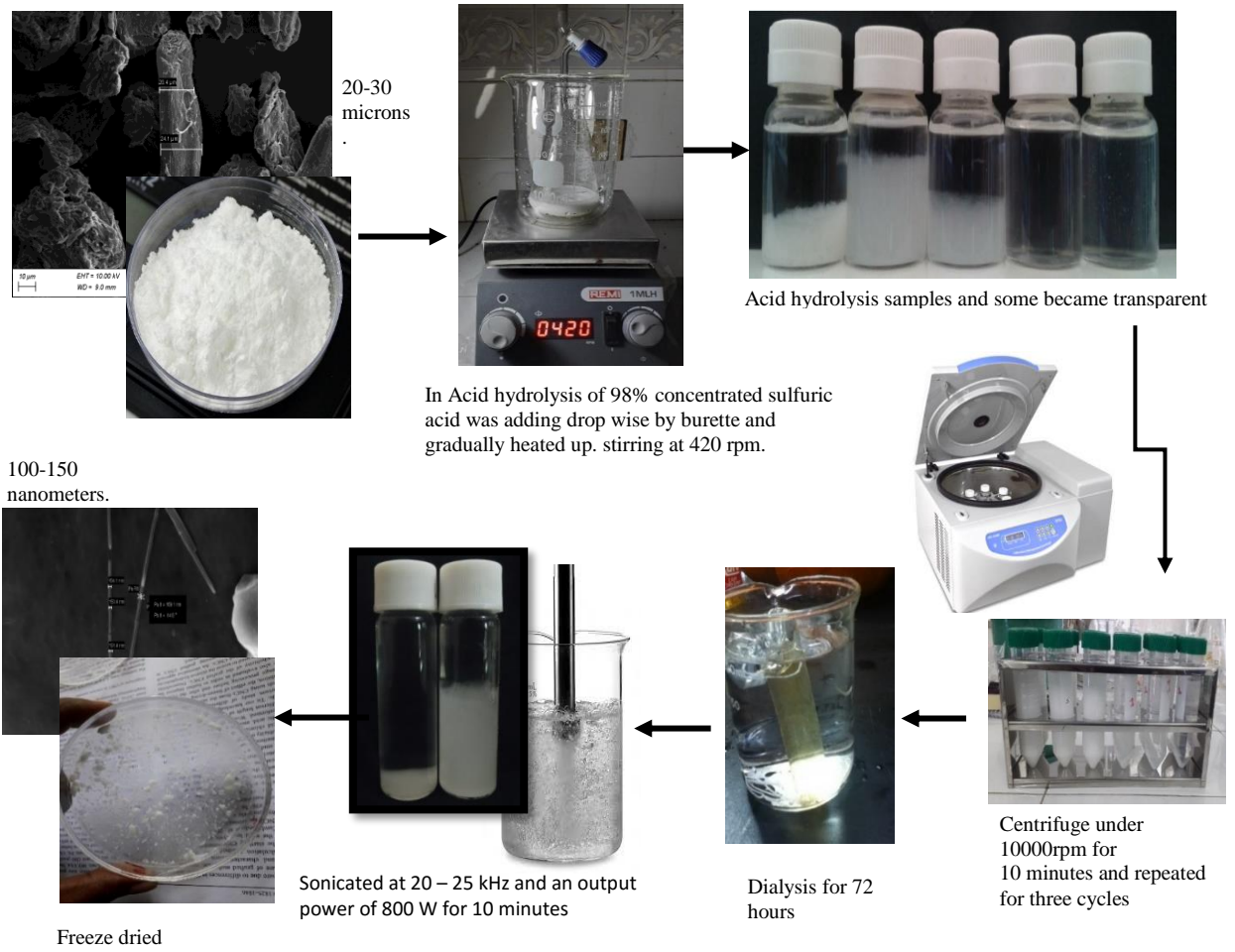


Figure 3: Preparation of MFC by using MCC as the starting material



Figure 4: Acid hydrolysis slurry of cellulose



Figure 5: Final freeze dried sample

## 4. Results and discussion

### 4.1. Analysis of the polyester amount in cotton/polyester fibre blend

In the textile industry generally cotton and polyester yarns are blended to create fabric with desired properties. There are two types of blends: CVC and PC. CVC stands for Chief Value of Cotton which is a cotton and polyester yarn blended fabric, whereby the amount of cotton fibre exceeds the amount of polyester fibres. Polyester and cotton fabric is termed PC is where the amount of polyester fibres exceed cotton fibres. According to the mixture ratio during the blending both cotton and polyester fibres are pass through the fibre plucking machine and then gradually undergo different types of cleaning machines and processes.

The homogenous fibre blending takes place at the fibre mixing machine. In this experiment the polyester and cotton fibres are mixed manually as per the predetermined weight ratios. We assume that it provides a homogenized cotton polyester blend as given by fibre plucking machine output. When observed, the FTIR in the wavenumber range 500–4000  $\text{cm}^{-1}$  a fingerprint range was found at the 1800-600  $\text{cm}^{-1}$  for the Polyester.

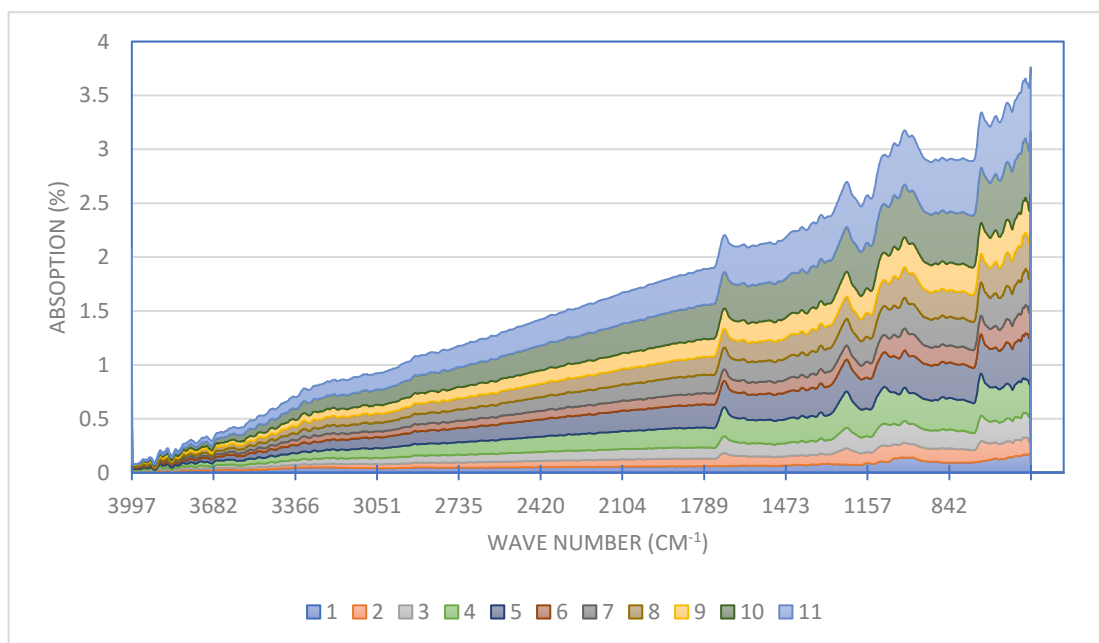


Figure 6: Characteristic absorption spectrums of cotton/polyester blended samples

Characteristic absorption peaks for the polyester and the cotton are summarized in the table below. The intensity of the absorption peaks varies with the amount of added polyester. The fingerprint range of 1800-600  $\text{cm}^{-1}$  for the polyester increased with the increasing amount of polyester content in fibre blend. The characteristic absorption peak at the 3435  $\text{cm}^{-1}$  that is responsible for the C=O stretching vibration overlaps the cotton OH stretching absorption peak in the spectrum.

Table 4: Identification of cotton polyester FTIR Wave number values [70]

Wavenumber ( $\text{cm}^{-1}$ )	Functional group(s)	Cotton	Polyester
3600-3500	OH, intermolecular H-bond	1	
3500-3300	Free OH str.	1	
3435	C=O str. (Overtone)		1
3059	C-H str. (C=C-H)		1
2974	C-H str. (-CH <sub>2</sub> -)	1	1
2910	C-H str. (-CH <sub>2</sub> -)	1	1
1740	C=O str.		1
1713	C=O str.		1
1649	O-H	1	
1612	C=C str. (ring C=C, C=C-C=C), C=O str.		1
1504	Skelton (aromatic ring), C=C str.		1
1433	O-H def.	1	
1412	C-H <sub>2</sub> sci., C-H <sub>2</sub> wagg.		1
1373	C-H <sub>2</sub> sci.	1	1
1346	C-H def.		1
1303	C-O str.		1
1240	Ether R-O-R asym. str.	1	1
1180	C-H str.	1	1
1142	C-H def.		1
1132	C-H <sub>2</sub> wagg., C-H <sub>2</sub> twist.	1	
1115	C-H def.		1
1093	C-H <sub>2</sub> twist	1	
1045	C-H <sub>2</sub> rocking	1	1
1004	C-O str. (alcohol C-OH)	1	
975	C-H bend (C=C-H)		1
898	C-H bend, C-H <sub>2</sub> rocking	1	1
873	C-H bend (ring puckering)		1
850	C-H bend (ring puckering)		1
795	C-H bend (ring puckering)		1
734	C-H <sub>2</sub> rocking		1



The characteristic absorption peak at 1740 cm<sup>-1</sup> and 1713 cm<sup>-1</sup> that is responsible for carbonyl group in the polyester is a very unique and strong vibration that is considered to be the fingerprint for the polyester. In some points like the absorption peaks at 2974 cm<sup>-1</sup> and 2910 cm<sup>-1</sup> which are responsible for the C-H stretching (-CH<sub>2</sub>-), 1373 cm<sup>-1</sup> that is for C-H<sub>2</sub> scission bond, 1045 cm<sup>-1</sup> that responsible for C-H<sub>2</sub> rocking vibration and at 898 cm<sup>-1</sup> corresponding to C-H bending are common peaks for both cotton and the polyester materials.

The cotton polyester blend ratios have been reflected in the absorption spectrum. The data for absorption spectrums in between 1800-600 cm<sup>-1</sup> range can be used to identify the mixture ratio of cotton and polyesters in the blends of the sample. FTIR derivative spectroscopic techniques were used to identify the hidden bands in the spectrum and subdue unwanted noises. It minimizes the unwanted deviations in the spectral bands like base line shifts, and enhances the significant difference between two spectrum bands. The absorption spectrum data that is obtained after second order derivative spectrum was subjected to Beer-Lambert law to obtain the mixture ratio of the cotton and polyester.

The Beer-Lambert law is constructed related to the attenuation property of the light when travelling through the material.

The absorption spectrum of a mixture of two compounds; polyester and cotton is determined by the equation of,

$$A_{m\lambda} = \xi_{m\lambda 1} C_A l + \xi_{m\lambda 2} C_B l \dots \dots \dots (3)$$

Where,  $A_{m\lambda}$  is the absorbance value of the mixture at wavelength  $\lambda_i$ ,  $\xi_{m\lambda 1}$  is the molecular absorptivity of Cotton and  $\xi_{m\lambda 2}$  is the molecular absorptivity of polyester.  $C_A$  is the amount of Polyester and  $C_B$  is the amount of Cotton in the cotton polyester blended sample.

One of the challenging points in this experiment is determining the necessary wavenumber range for analysis. The amount of polyester that is present in each sample gives the significant absorption peak copaired to the cotton in spectrum. These significant bands include the dominant characteristic peaks at 1713 cm<sup>-1</sup>-1740 cm<sup>-1</sup> that

is responsible for the carbonyl group,  $1346\text{ cm}^{-1}$  that is responsible for C-H  $\text{cm}^{-1}$  def,  $850\text{ cm}^{-1}$  and  $795\text{ cm}^{-1}$  for blending of C-H. This four absorption peaks are dominant for the polyester in the FTIR. The absorption peak at  $1740\text{ cm}^{-1}$  and  $1713\text{ cm}^{-1}$  that is responsible for the Carbonyl group in the polyester molecule was subjected to analysis. Figure no 7 shows the absorption spectrum of pure cotton and polyester. As shown in the figure, the polyester molecule gives the significant vibration of the two-carbonyl group C=O that is attached to the aromatic ring which give it a unique characteristic vibration in the broader spectrum. This original spectrum shows some unnecessary variations and notices.

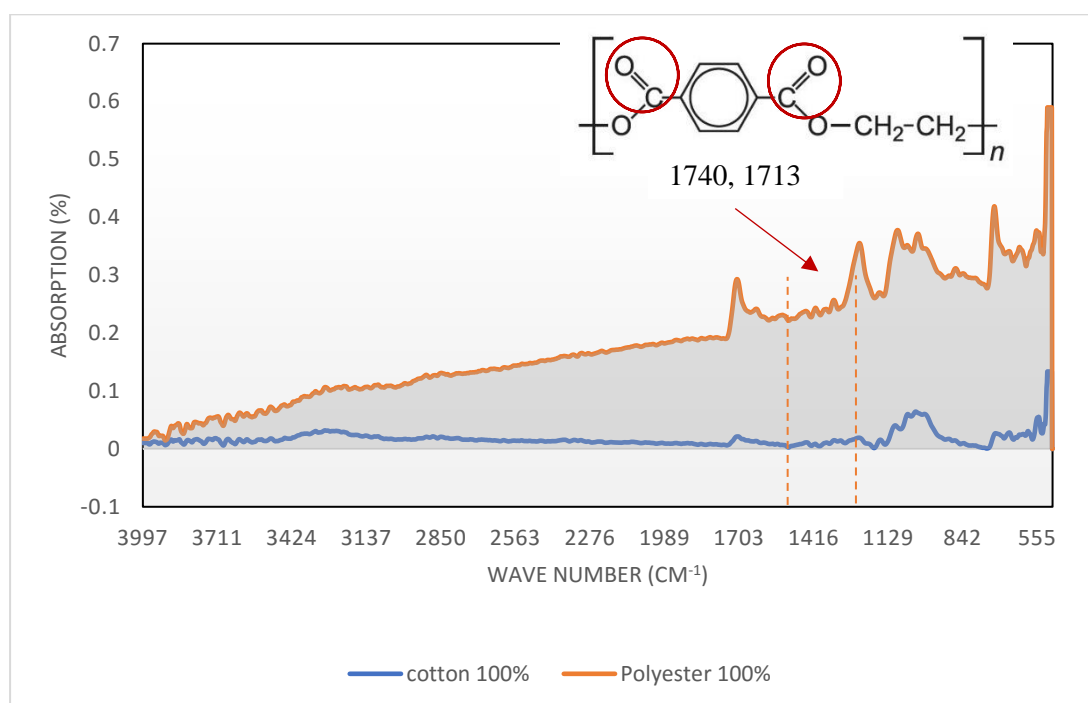


Figure 7: The FTIR spectrum of 100% cotton and the 100% polyester

The first derivative spectroscopy shown in figure no 8 lies in the wavenumber range of  $1573 - 1860\text{ cm}^{-1}$ . The first order spectrum obtained by  $dA/d\lambda$  vs  $\lambda$ , removes some of the unwanted variation and background noises of the spectral band but it requires additional processing steps to improve the separation of each spectrum from one another. Therefore, the second order derivative spectroscopy was obtained by

$d^2A/d(1/\lambda)^2$  vs  $\lambda$ . The second-order derivative spectrum as shown in figure no 20, eliminates most of the background noises and the bands are considerably separate from one another.

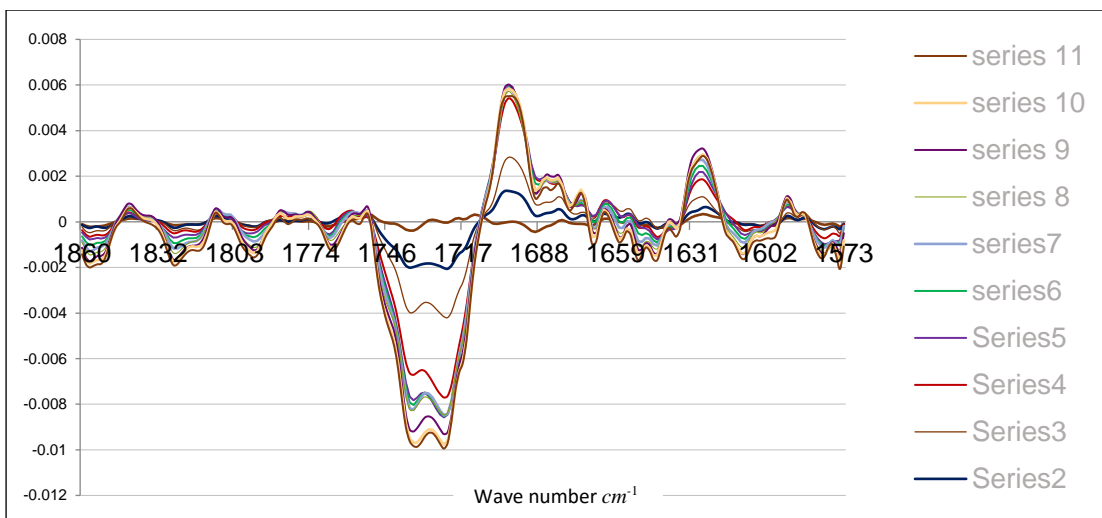


Figure 8: The FTIR first-order derivative spectrum wavenumber range of 1573 - 1860  $cm^{-1}$ .

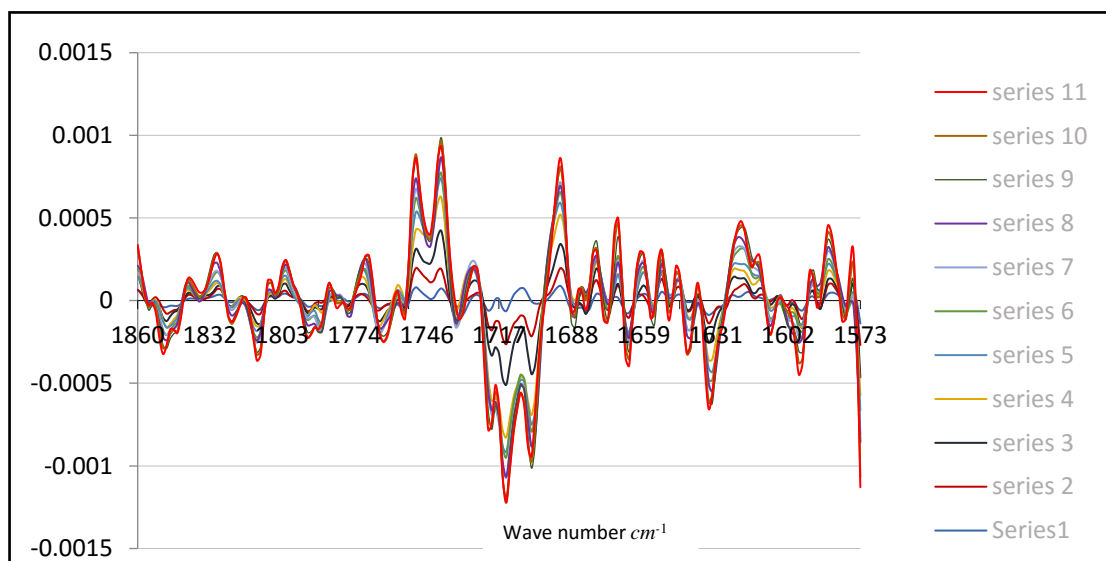


Figure 9: The FTIR second order derivative spectrum wavenumber range of 1573 - 1860  $cm^{-1}$

In the second-order, derivative spectroscopic height of the peak at the particular wave number was taken as the quantitative data that is corresponding to the amount of

polyester. The height of the peak identifies as the value of  $D_L$ . Table no 5 represents the summary of the data taken from the first and second-order derivative spectroscopy.

The first-order derivative spectroscopy summary shows that the series 5, series 6 and the series 7 overlap in the peak location of  $1740\text{cm}^{-1}$ . So, the peak heights are almost similar at the  $1740\text{cm}^{-1}$ . Compared to the first-order derivative spectroscopic data, the second-order derivative spectroscopy gives the most reliable data set that didn't make any overlaps in the particular wave number. The spectral bands are fairly separate and obtained clear values to  $D_L$ . The results were then use to obtain the equation to determine the composition ratio in accordance with Beer-Lambert Law.

$$A_{m\lambda}^0 = \xi_{m\lambda}^0 C^0 l \dots\dots\dots (5)$$

According to Beer-Lambert's law the absorbance  $A$  is expressed in terms of extinction coefficient  $\xi$ , the concentration of polyester  $C$  and the light path length of  $l$ . As a practice, the absorbance of the light is measured by the absorption spectroscopy at a constant wavelength. Here the light path length of  $l$  is considered as fixed. When the amount of polyester present in the mixture blend is known in advance, the term of extinction coefficient is obtained by a graph plotted by absorption vs amount of polyester.

The graph of the absorption vs amount of polyester that is plotted using the first derivative spectroscopic data is shown in figure 10. The blue dots represent the measured  $D_L$  values for each standard cotton/polyester blended sample. The straight blue line is the least- squares fitted line to the absorption vs amount of polyester content. In an ideal situation, the fitted straight line that is given by the data needs to go through the middle of the blue dots. The plotted equation of the fitted line that is  $X$ = the amount of polyester,  $f(x)$  is the absorbance and the value of  $R^2$  is a measure of the degree of correlation between the two values of amount of polyester and the absorption. (if the  $R^2$  value is closer to the 1.000 it gives the perfect correlation. Anything less than the 1.000 doesn't give the perfect correlation). In the first-order derivative spectroscopic graph the value of degree of correlation  $R^2$  is given as 0.7794. This situation is due to

Table 5: Summary of the FTIR spectroscopic data for polyester in each series.

<b>First -order derivative spectroscopy</b>				
<b>Sample no.</b>	<b>Wavenumber</b>	<b>Height of the peak (D<sub>L</sub>)</b>	<b>Polyester amount (g)/10g</b>	<b>Ratio given by model</b>
Series 1	1740	0.000	0	0.00
Series 2	1740	0.0024	1	0.24
Series 3	1740	0.0031	2	0.31
Series 4	1740	0.0063	3	0.63
Series 5	1740	0.0073	4	0.73
Series 6	1740	0.0075	5	0.75
Series 7	1740	0.0078	6	0.78
Series 8	1740	0.0061	7	0.61
Series 9	1740	0.0078	8	0.78
Series 10	1740	0.0081	9	0.81
Series 11	1740	0.01	10	1.00
<b>Second order derivative spectroscopy</b>				
<b>Sample no.</b>	<b>Peak location</b>	<b>Height of the peak (D<sub>L</sub>)</b>	<b>Polyester composition (g)</b>	<b>Ratio given by model</b>
Series 1	1740	0.00009	0	0.01
Series 2	1740	0.00012	1	0.13
Series 3	1740	0.0002	2	0.22
Series 4	1740	0.00031	3	0.34
Series 5	1740	0.00042	4	0.46
Series 6	1740	0.00051	5	0.56
Series 7	1740	0.00062	6	0.68
Series 8	1740	0.00071	7	0.78
Series 9	1740	0.00079	8	0.89
Series 10	1740	0.00089	9	0.98
Series 11	1740	0.00091	10	1.00

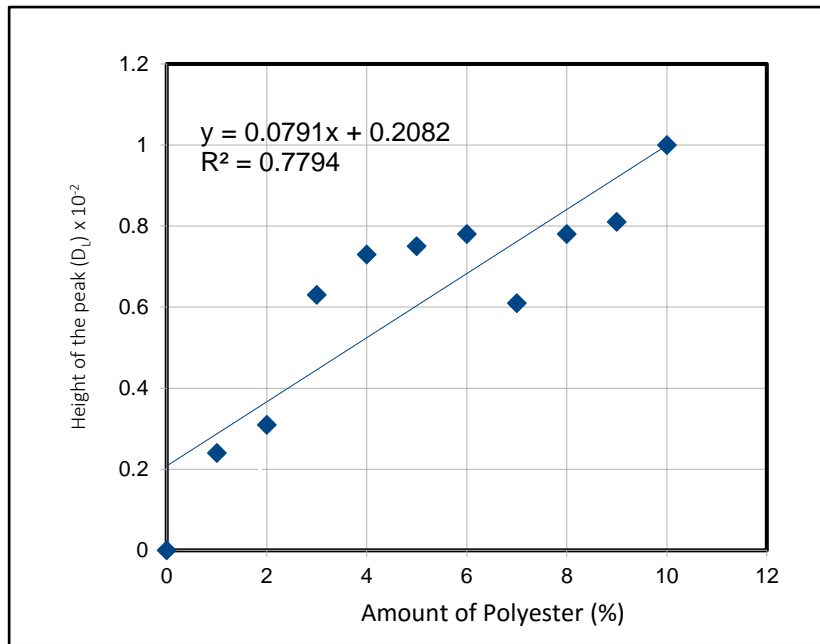


Figure 10: Absorption versus amount of polyester present in fiber blend

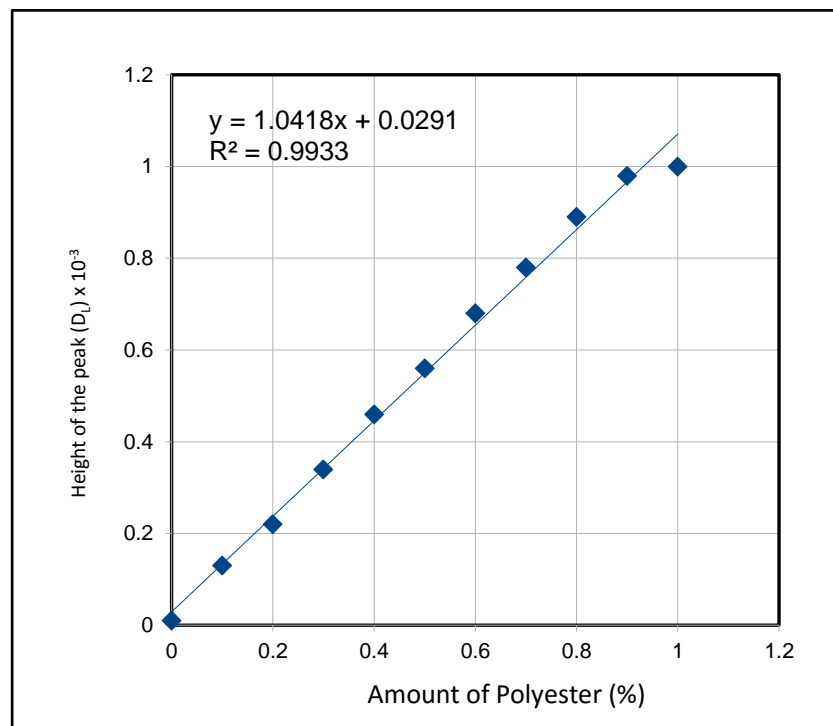


Figure 11: Absorption versus amount of polyester present in fiber blend

the spectral band overlapping in some points. This deviation was minimized drastically in the second-order derivative spectrum. The absorption vs amount of polyester present graph by second order derivative spectroscopy data is shown in figure no 11 and the degree of correlation  $R^2$  is 0.9933. It is revealed that the spectrum data is closer to the ideal situation. So, the prediction power of the percentage of polyester is higher in the second graph. The extinction coefficient is  $\xi = 1.0418$ . The equation for the composition of the polyester cotton blend is  $Y$  (absorption) =  $1.0418 X$  (Amount of polyester present).

## 4.2. Waste cotton fabric characterization

### 4.2.1. Moisture content of the waste cotton fabric

Table 6: The moisture content of the waste cotton fabric

Fabric samples mass (g)	Oven dry constant weight under 105 °C (g)	Moisture content (g)
10.02	9.91	0.11
10.01	9.93	0.08
10.02	9.94	0.08
10.02	9.91	0.11
10.01	9.94	0.07

The average moisture content of the raw material was 0.9 (wt%).

### 4.2.2. Ash content of the waste cotton fabric

Table 7: The Ash content of the waste cotton fabric

Initial weight (g)	residue weight (g)	Ash content (wt%)
10.03	0.148	1.479
10.02	0.148	1.479
10.03	0.149	1.489
10.01	0.147	1.469
10.00	0.149	1.490

Cotton contains rather low amounts of inorganic components, measured as ash. Typical deposits in the cell walls are various salts, such as carbonates, silicates, oxalates, and phosphates. The ash content of the sample is 1.48%.

### 4.3. Waste cotton fabric and raw cotton linters – FTIR analysis

Cotton comprises of a high amount of cellulose including trace amount of Hemi-cellulose, pectin and some waxes. Figure 12 shows the FTIR for raw cotton linters and the waste cotton fabric. Both spectrums follow the same patterns. All the characteristic peaks that are responsible for the cellulose are present in both spectrums. When comparing cotton linters and cotton cellulose the transmittance band that corresponds to OH stretching at  $3650\text{-}2900\text{ cm}^{-1}$ , peak attributed to the vibration stretching of  $\text{CH}_2$  at  $1430\text{ cm}^{-1}$ , CH bending at  $1370\text{ cm}^{-1}$ , OH bending vibration at wave number of  $1335\text{ cm}^{-1}$  and  $\text{CH}_2$  rocking vibrations at  $734\text{ cm}^{-1}$  intensities are slightly reduced.

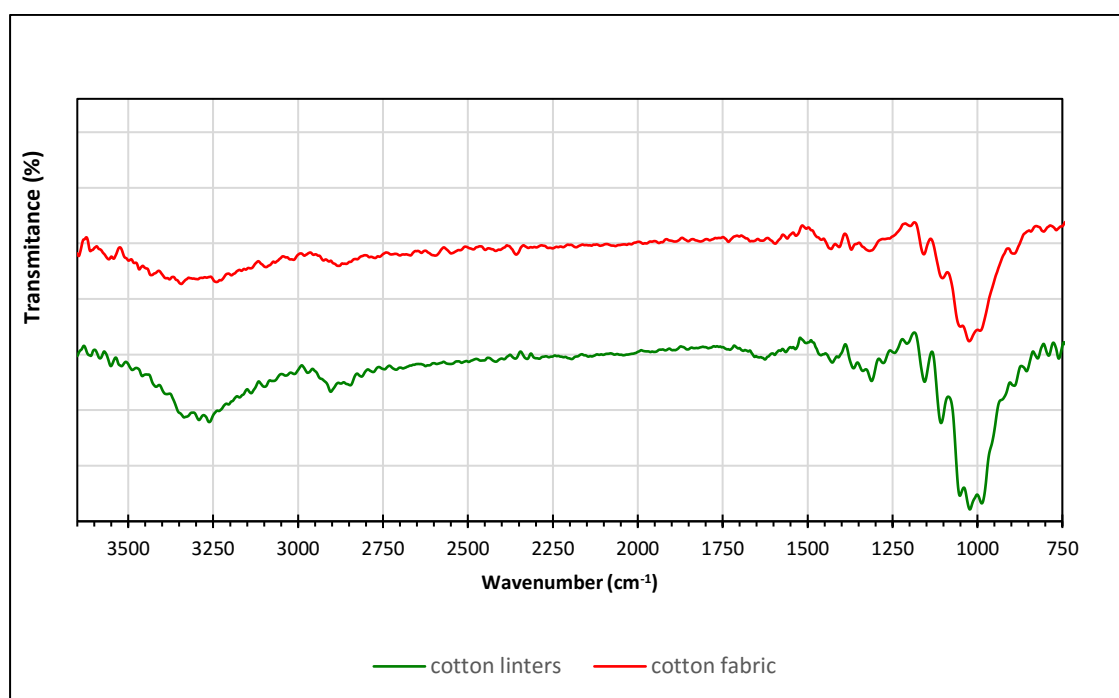


Figure 12: FTIR spectra of celluloses present in the cotton linters and the cotton fabric

This slight difference may be due to the aging of cotton. Cellulose in the cotton fabric can be subject to degradation due to many reasons during their processing steps. On a



molecular level, cotton fabric laundering and drying create a harsh environment for the cellulosic fibres and cause a reduction in the degree of polymerization. When the fabrics are laundered with detergent, the alkaline condition degrade the molecules at the end of the polymer chain. The cellulose molecules also undergo a peeling reaction in the alkaline condition.

#### 4.4. XRD analysis of waste cotton fabric and cotton linters

Cellulose is a linear polymer that has  $\beta$ -D-glucose units, linked by  $\beta$  (1 $\rightarrow$ 4)-glucosidic bonds and shows high molecular weight. The OH groups that are in the polymer chains have undergone large amount of inter and intra bonds that finally form ordered crystal structures. Each type of cellulose has well defined XRD patterns corresponding to their crystal structure. Therefore, XRD analysis was conducted to identify the content of cellulose I in the cotton fabric as well as to confirm the degree of crystallinity.

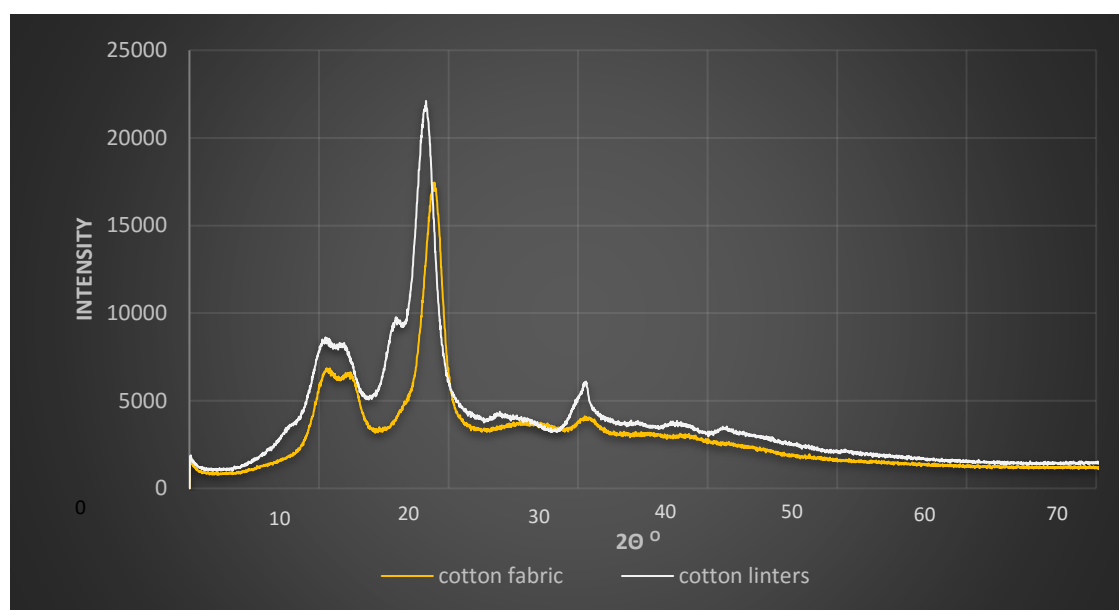


Figure 13: X-ray diffraction patterns of raw cotton linters and cotton fabric

Three peaks at  $2\theta = 14.36^\circ(110)$ ,  $16.28^\circ(110)$  and  $22.38^\circ(200)$  confirm that the presence of cellulose I in both cotton linters and the cotton fabric samples[32]. The crystallinity index of the raw cotton linters was 36 %, whereas the crystallinity index of cotton fabric was 32%. The degree of crystallinity value was reduced in the cotton

fabric compared to the cellulose in the cotton linters. This can occur due to the pre-treatment and purification of fabric yarns.

#### 4.5. TGA analysis of waste cotton fabric and cotton linters

The dehydration and thermal degradation behaviour of the cotton fabric and the linters were characterized through thermogravimetric analysis (TGA). Specimen of 5-10 mg were tested in a temperature range 25 to 400 C°. The thermal decomposition pattern is almost the same for both the cotton linters and cotton fabrics. Many studies related to the thermal decomposition of cellulose can found in research literature. The second significant thermal decomposition of Cellulose started at 320 °C and continued up to 400 °C while maximum weight loss can be observed at 335 °C. Usually the Cellulose associate hemicellulose starts to decompose at 220°C and remains up to 315 °C.

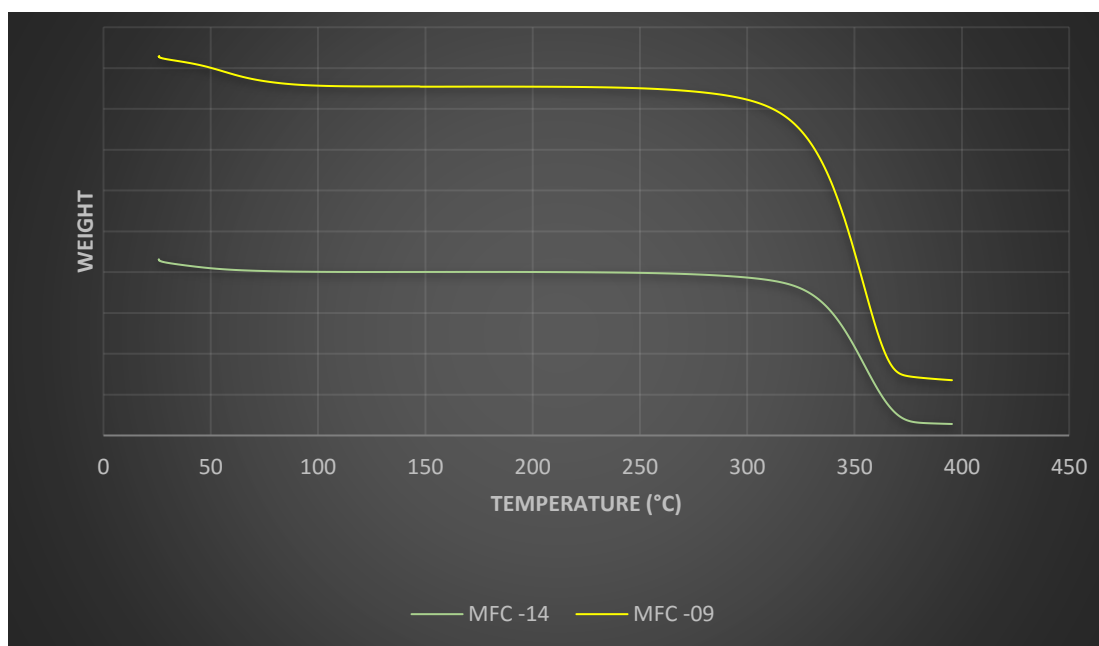


Figure 14: TGA curve for cotton linters and the waste cotton fabric

#### **4.6. Experimental design to optimized the acid hydrolysis parameters**

The efficiency of the acid hydrolysis towards extraction of MFC is dependent on factors that include;  $X_1$  -  $H_2SO_4$  Concentration,  $X_2$  - Hydrolysis time and  $X_3$  - Temperature. This experiment was designed to optimize the effect of these three independent factors on two responses including the Width  $Y_{size}(nm)$  and Yield  $Y_{yield}(\%)$  of the cellulose fibres. The Response surface methodology was employed to determine the effect of experiment. To construct the experimental design Box-Behnken model was used since it involves a minimum number of samples. The Box-Behnken method is an individualistic quadratic design and it does not contain any factorial design. The Box-Behnken model gives the treatment combinations at the edges of the process space and the mid points of the edges and at the centre point and does not give any axial points itself. Therefore, this experiment was designed to get realistic data. 15 experimental runs were conduct with the three levels of parameters as mentioned in the methodology. At the middle points that is coded as 0 was replicated thrice to determine the repeatability of the experiment. The two responses of yield of the MFCs and the width of the fibres measured after all the samples were freeze dried. As the target is to destructively reduce the amorphous domain of the cellulose and decrease the size of the cellulose fibre, the most reduced sizes of four samples were taken for further instrumental analysis.

Therefore, the MFCs yield and the width of the particles were used as the dependent variable of the ANOVA statistical test. The ANOVA statistical test results were used to determine the significance of the main parameter effect on the effective hydrolysis process. The effective hydrolysis parameters were determined by sufficient acid concentration to remove the amorphous part of the cellulose, and the penetration power in to the inner cellulosic matrix depended upon the temperature of the reaction mixture and the time.

#### **4.7. Development of the regression model**

Two regression models were used in two dependent responses – the width of the cellulose fibres and the yield. In the experiment, the model selection was done based on the highest order polynomial. The statistical analysis was completed using MINITAB 2018 software. Full quadric model was selected to give both responses since full quadric model gives the highest flexibility.

The coefficient of the linear terms of three experimental factors including; ( $X_1$ )  $H_2SO_4$  Con, ( $X_2$ ) Hydrolysis time and ( $X_3$ ) Temperature shows the highest affected factors of extraction of MFCs. The interaction of each factors was then obtained by multiplying the two coefficient factors as  $X_1 X_2$ ,  $X_2 X_3$  and  $X_1 X_3$ . Second-order interaction was also determined by the combination of factor effect including,  $X_{12}$ ,  $X_{22}$  and  $X_{32}$  that represents the quadric effect on the responses. Finally, the equation was obtained in both the width and the yield of the MFCs by optimizing these three parameters.

#### 4.8. ANOVA analysis and lack-of-fit

The three factor levels of lower, middle and upper level with the coded value and natural values are given in the table no 8 mentioned below. The experimentally obtained yield and the width values were used to analyse the variance. The accuracy of the experimental model that was developed to optimize the parameter of the hydrolysis process in extraction of MFC was validated.

Table 8: Independent variable used for the experiment and their coded values

Independent variable	Unit of variable		Coded values		
			-1	0	+1
$H_2SO_4$ Con.	w/w	$X_1$	48	52	56
Hydrolysis time.	min	$X_2$	10	65	120
Temperature.	$^{\circ}C$	$X_3$	40	60	80

In the model fitted, both regression coefficients or  $R^2$  value and the F-value that was generated from the software was used to justify the validity and the significance of the practically obtained values in the experiment. In total, fifteen samples were utilized to determine the nine regression coefficients in extraction of MFC. Table no 9 below represents the regression coefficient values including factor interactions. The model fitting is very important to get reliable information, in optimizing the respond surface as misaligned results leads to poor fitting.

The quadratic model that was selected by the software for the width of MFC can be represented by the equation given below. The positive sign represents the synergetic effect and the negative sign represents the antagonistic effect on each factor. The coefficient of each factor of acid concentration, hydrolysis temperature and time on the effect of acid hydrolysis of MFCs and the coefficients with two factors in second-order interaction terms gives quadratic effect.

Table 9: ANOVA statistical analysis and the lack-of-fit test results for width of the MFC

Source	Degree of freedom	Sum of squares	Mean Square	F-Value	P-Value
Model	9	805781	89531	25.71	0.001
Linear	3	683387	227796	65.42	0.000
Concentration	1	649230	649230	186.45	0.000
Time	1	30876	30876	8.87	0.031
Temperature	1	3280	3280	0.94	0.376
Square	3	120061	40020	11.49	0.011
Con.*Con.	1	49934	49934	14.34	0.013
Tim*Tim	1	44036	44036	12.65	0.016
Tem*Tem	1	17813	17813	5.12	0.173
2-Way Interaction	3	2333	778	0.22	0.876
Con.*Tim	1	992	992	0.28	0.016
Con.*Tem	1	441	441	0.13	0.036
Tim*Tem	1	900	900	0.26	0.633
Error	5	17410	3482		
Lack-of-Fit	3	17350	5783	190.66	0.005
Pure Error	2	61	30		
Total	14	823192			

Table 10: Modal summary

SD	Correlation Coefficient, R <sup>2</sup>	Adjusted R <sup>2</sup>
59.0092	97.89%	94.08%

$$\begin{aligned} \text{Mean Width (nm)} &= 436.3 - 284.9 \text{ Con.} + 62.1 \text{ Tim} - 20.2 \text{ Tem} - 116.3 \text{ Con.} \times \text{Con.} \\ &\quad + 109.2 \text{ Tim} \times \text{Tim} + 69.5 \text{ Tem} \times \text{Tem} + 15.8 \text{ Con.} \times \text{Tim} - 10.5 \text{ Con.} \times \\ &\quad \text{Tem} - 15.0 \text{ Tim} \times \text{Tem} \end{aligned}$$

The model accuracy can be validated by the R<sup>2</sup> value, adjusted R<sup>2</sup> and standard deviation. The ratio between the sum of square and the total sum of square gives by R<sup>2</sup> value totally explains the model estimation reliability on the experiment data. R<sup>2</sup> value

that was given for the width was 97.89% and adjusted  $R^2$  was 94.08%. The experimental data shows better fit for that of the MFCs. Figure no 16 shows that the significance of three factors of acid concentration, hydrolysis time and the temperature effect on the mean width of the MFCs.

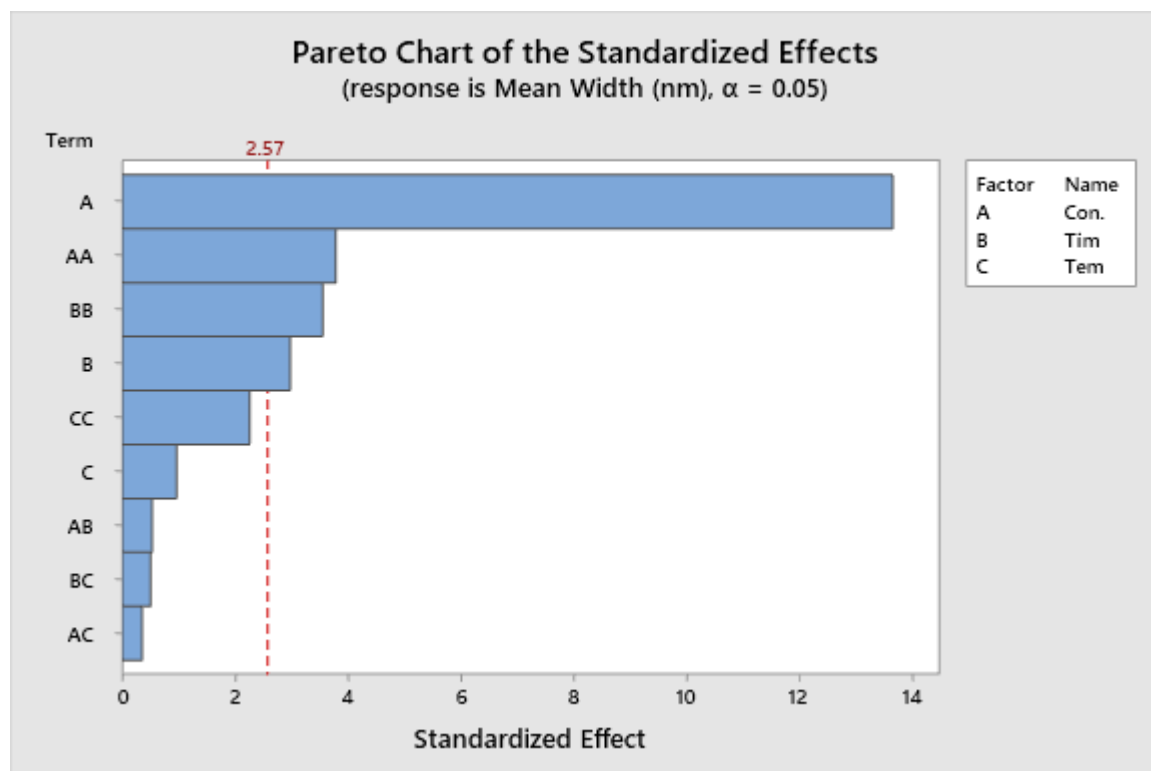


Figure 15: Parato chart of standardized effect of concentration, time and temperature on width of MFCs

The model F-value was recorded as 25.71 and the value of p was 0.01 which shows that the model was significant. According to the ANOVA results, the effect of acid concentration and time is significant to the mean width of the cellulose fibres with a significant level of  $\alpha < 0.05$ . Therefore, the Con. Time was the significant model terms to the width of MFC. The Results of ANOVA demonstrate the response of yield of MFC as shown in table no 11. The sulfuric acid concentration and acid hydrolysis temperature are significant model terms on the yield.  $R^2$  value that was given for the width was 98.42% and adjusted  $R^2$  was 95.58%. The experimental data shows better fit for the MFC yield. The p value of concentration and time is almost 0.00 which means

that those two factors are significant. Figure no 17 shows the significance of the three factors of acid concentration, hydrolysis time and the temperature on the yield of the MFCs. The acid concentration, time and temperature are significant on the yield of MFC.

Table 11: the ANOVA statistical analysis and the lack-of-fit test results percentage yield of the MFC.

Source	Degree of freedom	Sum of squares	Mean Square	F-Value	P-Value
Modal	9	290.933	32.326	34.63	0.001
Linear	3	182.000	60.667	65.00	0.000
Concentration	1	162.000	162.000	173.57	0.000
Time	1	2.000	2.000	2.14	0.203
Temperature	1	18.000	18.000	19.29	0.007
Square	3	39.933	13.311	14.26	0.007
Con.*Con.	1	21.564	21.564	23.10	0.005
Tim*Tim	1	4.333	4.333	4.64	0.084
Tem*Tem	1	13.564	13.564	14.53	0.012
2-Way Interaction	3	69.000	23.000	24.64	0.002
Con.*Tim	1	1.000	1.000	1.07	0.348
Con.*Tem	1	4.000	4.000	4.29	0.033
Tim*Tem	1	64.000	64.000	68.57	0.000
Error	5	4.667	0.933		
Lack-of-Fit	3	4.000	1.333	4.00	0.206
Pure Error	2	0.667	0.333		
Total	14	295.600			

Table 12: Model summary

SD	Correlation Coefficient, R <sup>2</sup>	Adjusted R <sup>2</sup>
0.96609	98.42%	95.58%

$$\text{yield\%} = 27.333 - 4.500 \text{ Con.} + 0.500 \text{ Tim} - 1.500 \text{ Tem} - 2.417 \text{ Con.} \times \text{Con.} + 1.083 \text{ Tim} \times \text{Tim} - 1.917 \text{ Tem} \times \text{Tem} + 0.500 \text{ Con.} \times \text{Tim} + 1.000 \text{ Con.} \times \text{Tem} - 4.000 \text{ Tim} \times \text{Tem}$$

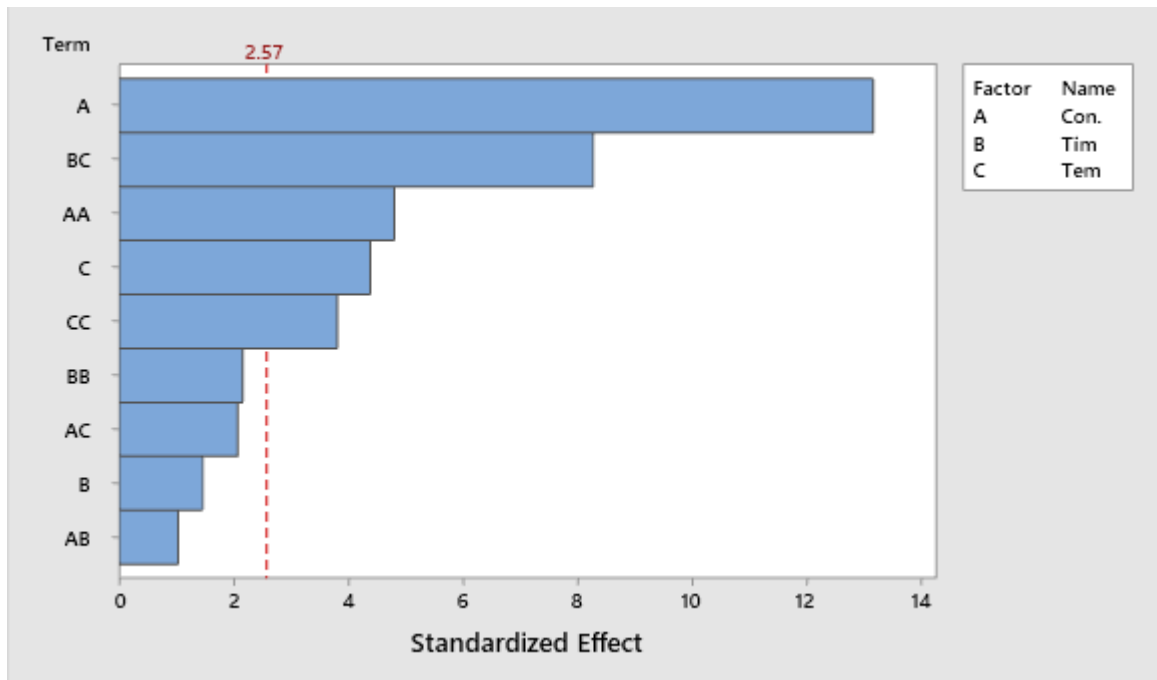


Figure 16: Pareto chart of standardized effect of concentration, time and temperature on yield of MFCs (response is yield (%),  $\alpha = 0.05$ )

#### 4.9. Process Variables Optimization

Base on the experimental data the acid hydrolysis process was optimized to obtain a higher yield and a lower width of MFC. The optimum surface was created by using software. The criteria applied hereto in order to obtain the respond surface is to maximize the yield and minimize the width of the MFC. When the model lack-of-fit shows as significant, the regression equation for both yield and the width are reliable. Those two regression models are sufficient to predict the effect of the three parameters on the extraction of MFC. The relationship between the factors and the responses are illustrated in the three-dimensional surface plot and two-dimensional contour plots.



#### 4.10. Contour Plots and surface plot of width of MFC

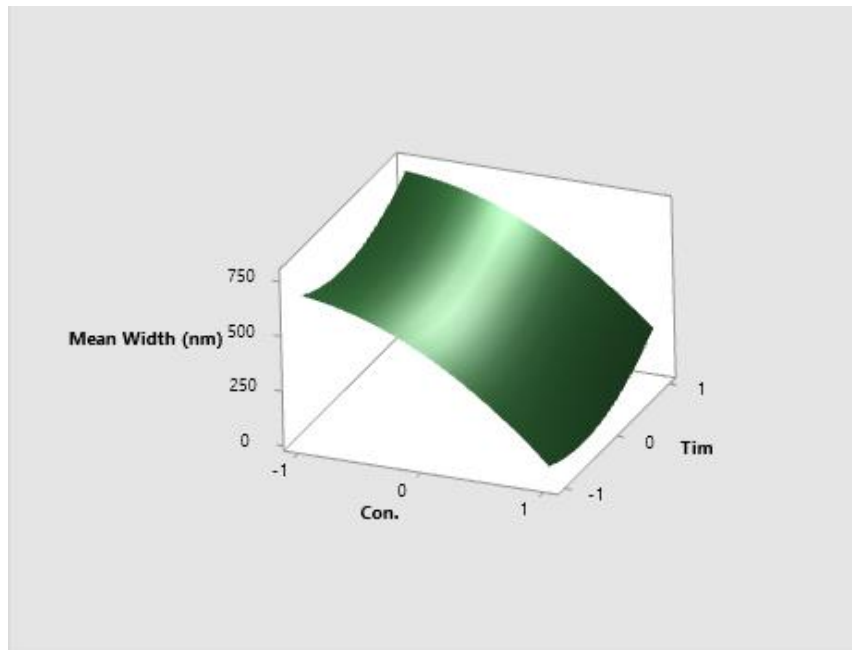


Figure 17: Surface plot of mean width vs. time and concentration (hold temperature)

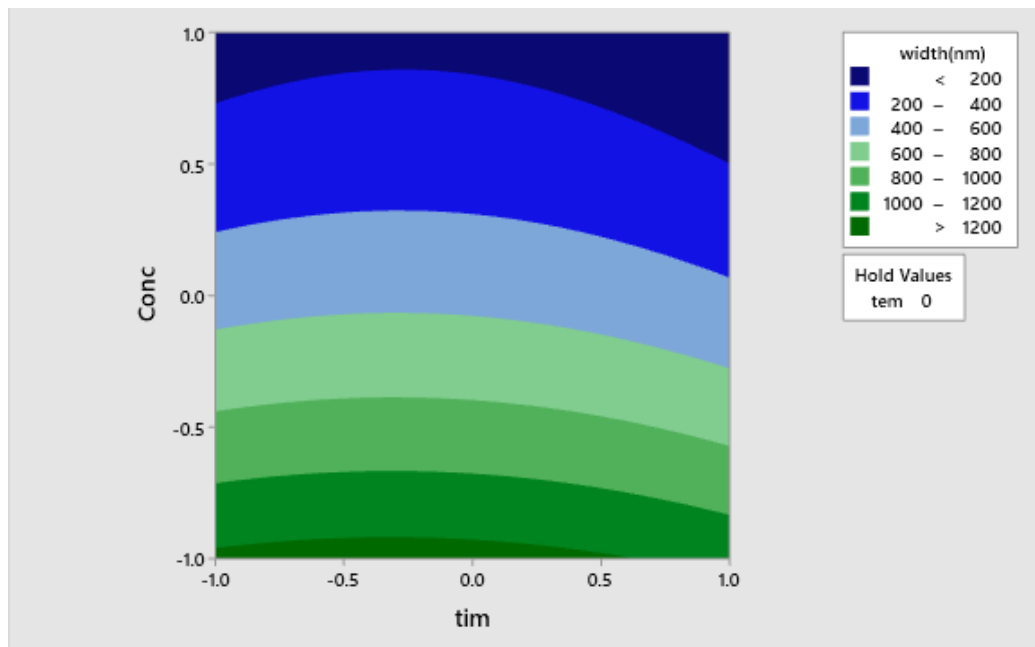


Figure 18: Contour plot of mean width vs. time and concentration (hold temperature)

The ANOVA statistical test results of width give p values of 0.3 and 0.033 for the two parameter effects of Concentration.Time and Concentration.temperature. Therefore, it was clear that concentration, temperature and time were two significant factors on width of cellulose fibres.

The three-dimensional surface plot of mean width vs. time and concentration was illustrated in figure no 18 where the temperature of the reaction mixture was kept as a constant in 60°C. Figure no 19 was a two-dimensional contour plot of two factors - time and concentration effect on the mean width. The width of the cellulose was drastically reduced when the sulfuric acid concentration was increased up to 56% (w/w) while keeping the reaction time in between 65-120 minutes. This synergistic effect on the width of the MFC was observed when the concentration increases with time. Therefore, when the concentration is increased, the width of the MFC is reduced. However, when the concentration is self-evidently increased the reaction time can be minimized as required. On the other hand, enhanced acid hydrolysis time lead to physical swelling of the cellulose fibres. Therefore, the surface area of the cellulose was increased which consequently leads to higher hydrolysis efficiency.

The three-dimensional surface plot of mean width vs. temperature and concentration was illustrated in figure no 20 where the time of the reaction mixture was kept as a constant at 65 minutes. Figure no 21 was a two-dimensional contour plot of two factors - temperature and concentration effect on the mean width. When the temperature and the concentration was increased, the width of the FMC was reduced. When the concentration was increased up to 56% (w/w) and temperature varied in-between 60-80°C, the width of the MFC was reduced to below 200nm. When the temperature of the medium increases, the diffusion power or the penetration ability of the reaction medium was increased. Therefore, the efficiency of acid hydrolysis is increased by reducing the amorphous domain in the cellulose fibres. For considering both time and the temperature with concentration it can clearly show that the hydrolysis power of the sulfuric acid was greatly increased by the temperature of the reaction mixture while the time of the reaction taking place needs to be maintained at a moderate value.

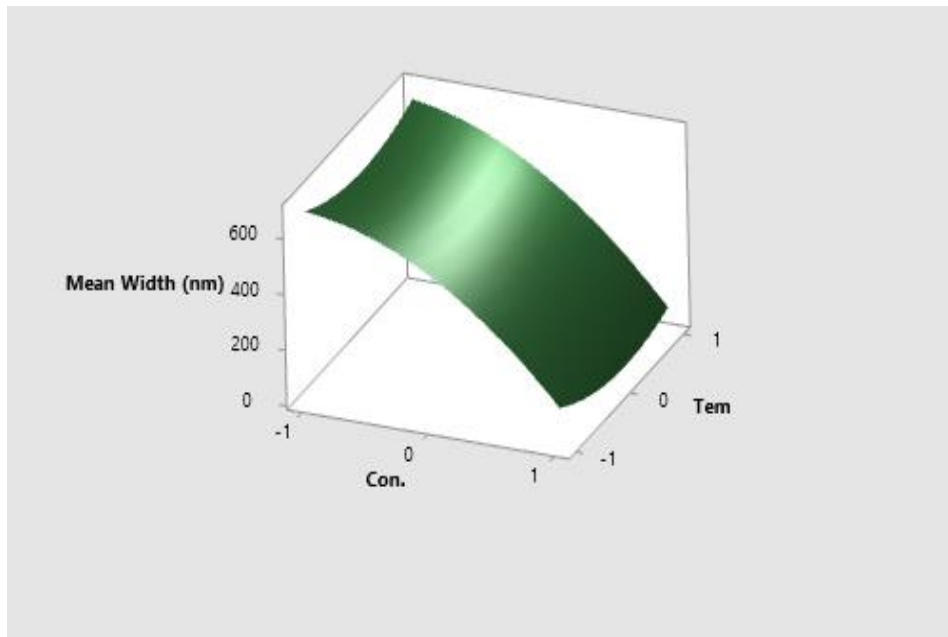


Figure 19: Surface plot of mean width vs. temperature and concentration (Hold time)

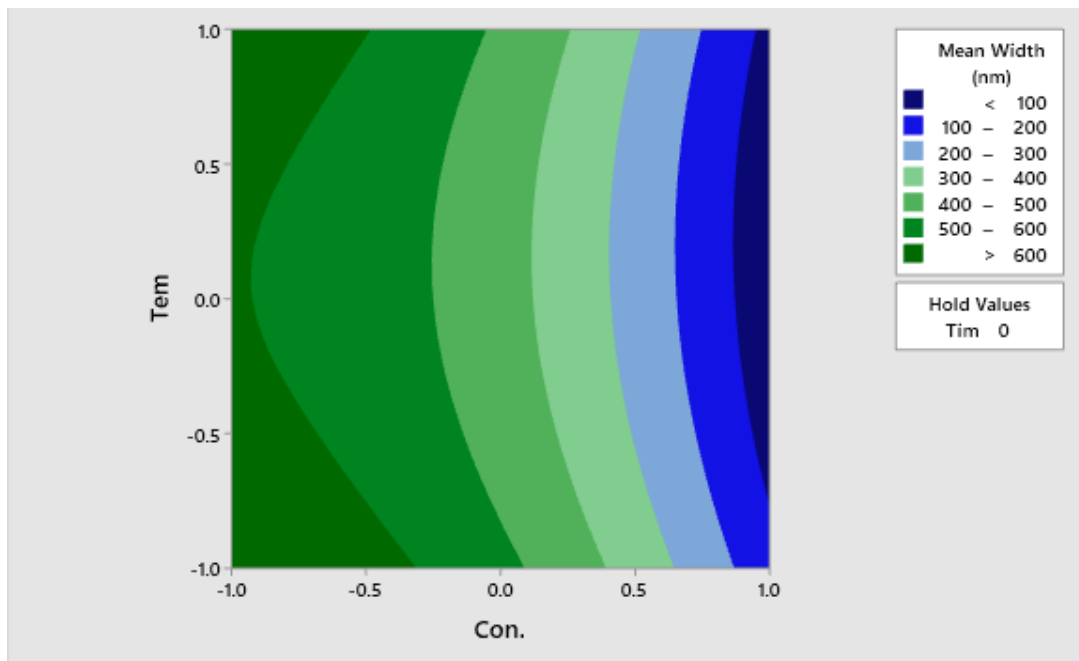


Figure 20: Contour plot of mean width vs. temperature and concentration (hold time)

#### 4.11. Contour plots and surface plot of Yield of MFC

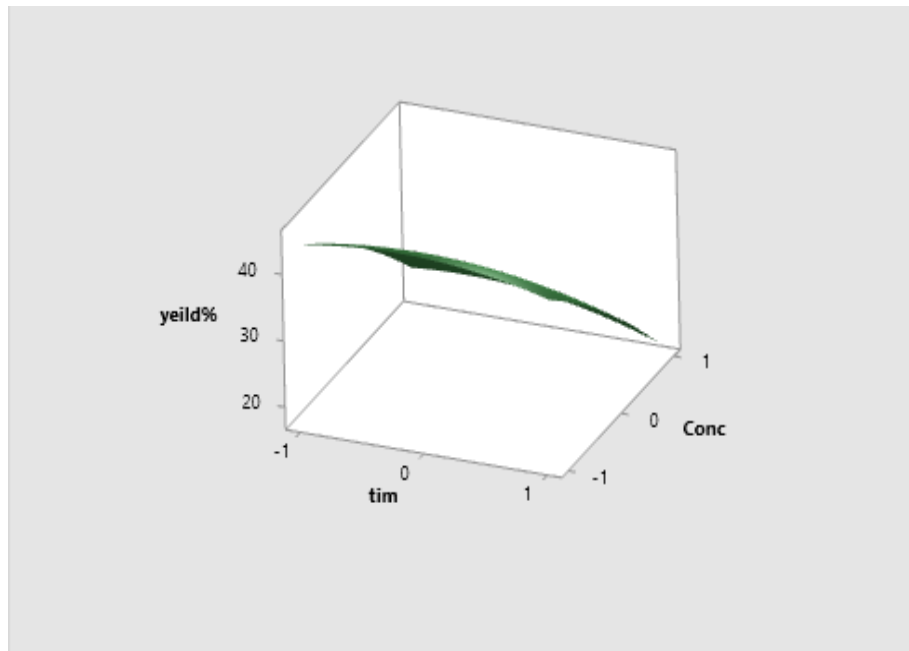


Figure 21: Surface plot of yield vs. time and concentration (hold temperature)

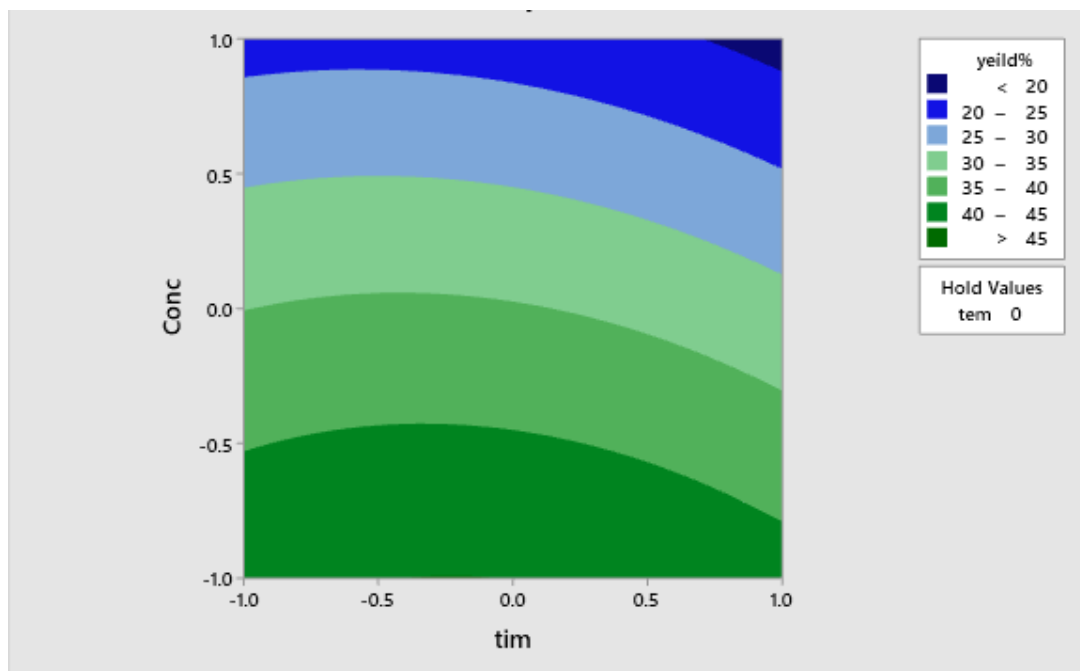


Figure 22: Contour plot of yield vs. time and concentration (hold temperature)

According to the ANOVA statistical test results of yield, the p values of the two parameter effects of Concentration. Time was 0.016, Concentration. temperature was 0.036 and Time. Temperature was 0.633. Therefore, it was clear that Concentration. Time and Concentration temperature were two significant factors on acid hydrolysis process yield.

Figure 22 surface plot of yield was constructed to illustrate the effects of concentration and time to the percentage of yield of the MFC, where the reaction temperature of the mixture was kept as a constant at 60<sup>0</sup>C. Figure 23 Contour plot of yield was used to depict the two-dimensional illustration that determines the relationship of the combined effects of two variables, hydrolysis concentration and time on the percentage of yield. The percentage of yield was decreased significantly when the concentration and time were increased. This is due to the rapid hydrolysis of the amorphous part of the cellulose when increase the concentration and temperature of the reaction mixture occurs.

Figure 24 depicts a three-dimensional surface plot of yield constructed to illustrate the effects of concentration and temperature to the percentage of yield. Figure 25 shows a counter plot where the reaction time of the reaction mixture is kept as a constant at 60 minutes. The percentage of yield decreased significantly when the concentration and temperature were increased. When the temperature increased the acid diffusion power significantly increased and reacted with the cellulose drastically which in turn, reduced the yield.

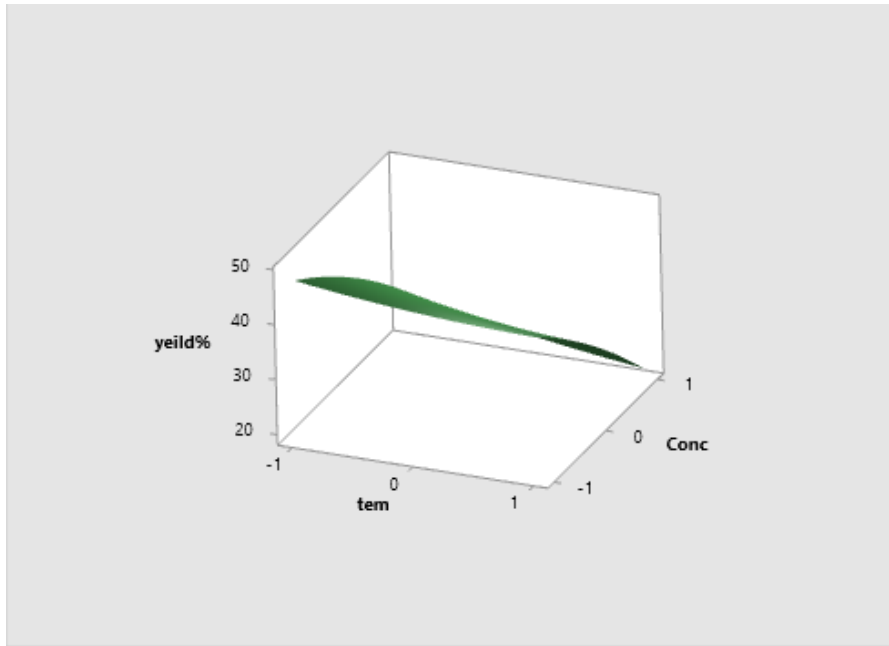


Figure 23: Surface plot of yield vs. time and concentration (hold time)

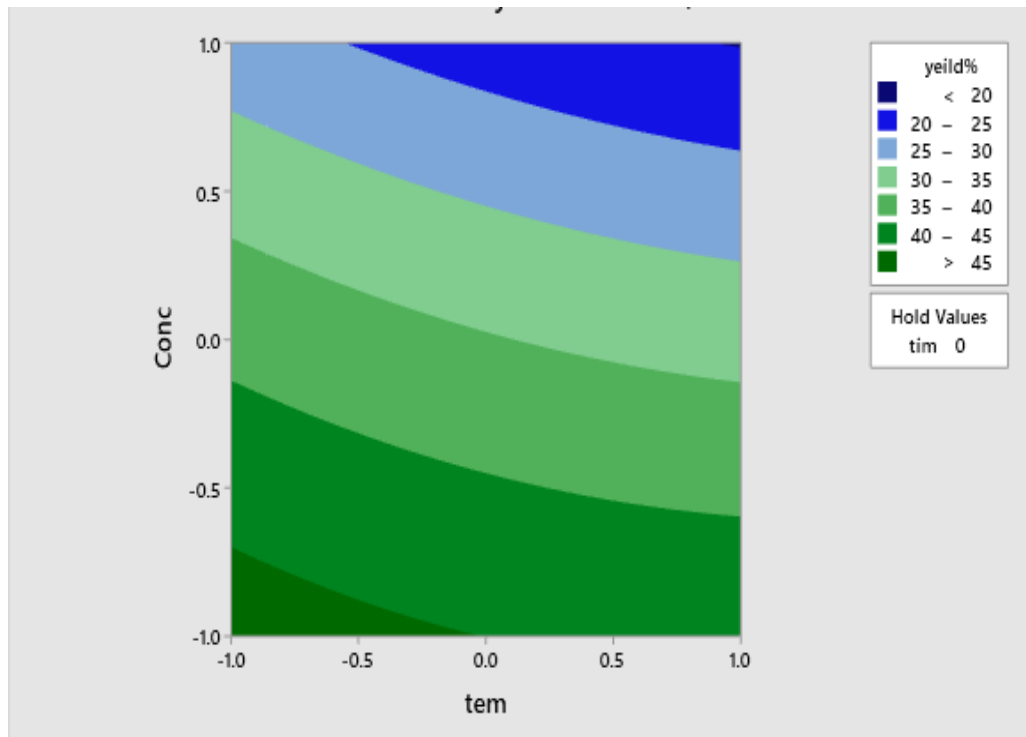


Figure 24: Contour plot of yield vs. time and concentration (hold time)

Hydrolysis of cellulose is of two types - one is acid hydrolysis and the other, enzymatic hydrolysis. For both types the concentration of the reactant, time and the temperature of reaction medium was significantly affected [42, 43]. These are influencing factors in energy transformation upon kinetics. Acid hydrolysis of cellulose is a complex chemical reaction that involves many physical factors. A small modification of the experimental factors lead to different pathways and speed. In research literature, it has been reported that the penetration power of the different acid concentrations directly affects the surface morphology of cellulose and physical properties like thermal degradation behaviour and the degree of crystallinity index [22]. Sulfuric acid is considered as a selective hydrolyzer of the amorphous domain of cellulose. Table 13 summarizes the best four samples giving the minimum value of mean width and their yield. These best four samples are then subjected to further analysis to determine the quality of each sample MFC.

Table 13: Microfibrilated cellulose samples that gives minimum values for the width.

<b>Sample</b>	<b>Concentration</b>	<b>Time</b>	<b>Temperature</b>	<b>Mean width(nm)</b>	<b>Mean yield%</b>
<b>MFC 2</b>	1	-1	0	340	20
<b>MFC 8</b>	1	0	1	140	18
<b>MFC 9</b>	1	1	0	245	22
<b>MFC14</b>	1	-1	-1	470	20

#### 4.12. FTIR Characterization of the MFC

Chemical functionality of the extracted microfabricated cellulose was examined by the FTIR spectroscopy. Main transmittance peaks are observed in two regions at 3660 - 2800  $\text{cm}^{-1}$  and 1650 -750  $\text{cm}^{-1}$ . Figure 26 below presents the FTIR spectra of MFCs from the sample MFC-2, MFC-8, MFC-9, MFC-14 respectively. All four samples follow the same pattern with slight differences in intensities of transmittance band peaks.

The identification of the FTIR characteristics peaks for the cellulose are as follows. The broad peak observed at 2900-3660  $\text{cm}^{-1}$ , is responsible for the OH and CH bonds vibrations in the polysaccharides. The repeating unit of polysaccharide contained three OH groups, these hydroxyl groups then form hydrogen bonds which decide the physical properties of the cellulose. The adjacent two anhydroglucose rings covalently bonded  $\beta$  1-4 glucosidic bond by C1 and C4 atoms of ring. This determines the linearity of the cellulose chain and the degree of the polymerization [69, 70, 71].

The broad peak at 3600-3000  $\text{cm}^{-1}$  that corresponds to the OH groups of intermolecular Hydrogen bonds in the polymer chain while the peak was observed at 3500-3300  $\text{cm}^{-1}$  corresponding to the free hydroxyl groups. The sharp peaks at 2974  $\text{cm}^{-1}$  and 2910  $\text{cm}^{-1}$  correspond to the C-H stretching vibration of hydro-carbon in the polymer chain. These two peaks separations can be clearly seen in the MFC-08 which is depicted in dark purple. The Van der Waals bonds and intermolecular hydrogen bonds formed by OH and O in the adjacent anhydroglucose rings bind cellulose chains together and are led to form microfibrils in cellulose [71-73]. FTIR spectrum band of MCF-8 in purple colour shows a broad peak at 3600-300  $\text{cm}^{-1}$  than the other three spectra. That is due to the OH groups introduced in the hydrolysis steps. The fingerprint region of the cellulose can be observed in the 1650 -750  $\text{cm}^{-1}$  regions. The typical peak observed at the 1633  $\text{cm}^{-1}$  corresponding to the absorbed water in cellulose. All four samples show the absorbed water as freeze drying does not remove the absorbed water completely.



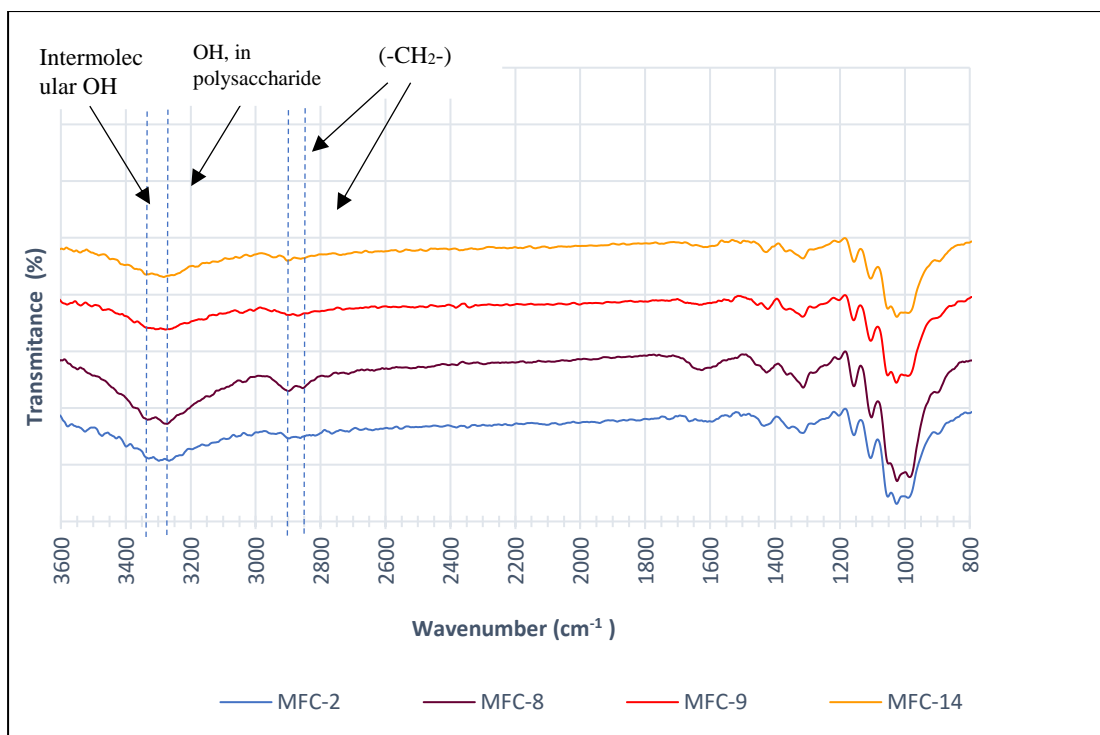


Figure 25: FTIR Spectrum of MFC samples

The peak observed at the  $1730\text{ cm}^{-1}$  that corresponds to the characteristic peak for C-O stretching vibration of  $\text{C}_2\text{H}_3\text{O}$  (acetyl) and ester linkages of hemicellulose totally disappears in this stage. Hemicellulose that are present in the cotton may be removed during the chemical pre-treatments of the cotton fibres. The transmittance peak at the  $1430\text{-}1420\text{ cm}^{-1}$  is due to the  $\text{CH}_2$  scissoring motion in cellulose. That is considered as a fingerprint of cellulose structure.

Figure 26 shows the fingerprint regions of the cellulose at  $1512\text{ cm}^{-1}$  to  $800\text{ cm}^{-1}$  for a clearer picture. The slight peak at  $1370\text{ cm}^{-1}$  that is attributed to the CH bending,  $1335$  and  $1320\text{ cm}^{-1}$  are attributed to the in-plane OH bending and  $\text{CH}_2$  wagging vibration. The dominant peak that gives at the  $1162\text{ cm}^{-1}$  corresponds to the C-C ring stretching vibration. The polysaccharide chain  $\beta$ -glycosidic linkages generate characteristic peak at  $902\text{-}893\text{ cm}^{-1}$  and the peak at  $1105\text{ cm}^{-1}$  attributes for the C-O-C glycosidic ether bond [71-73].

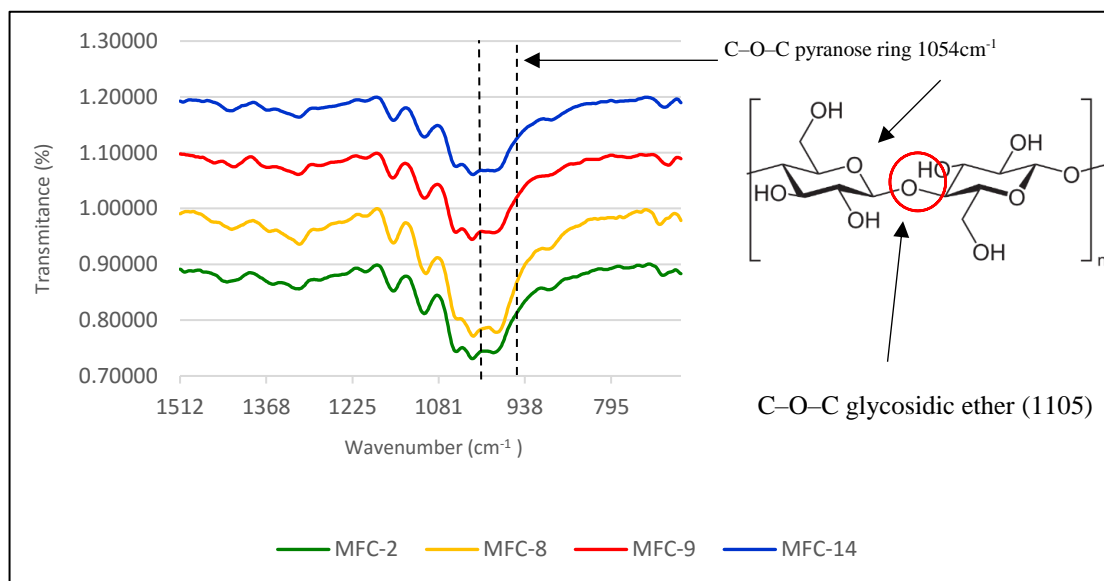


Figure 26: FTIR spectra of celluloses studied in the region between  $1512\text{ cm}^{-1}$  to  $800\text{ cm}^{-1}$

According to the literature reported, the FTIR spectral band at  $1427\text{ cm}^{-1}$  and  $897\text{ cm}^{-1}$  corresponds to the native cellulose I content and this spectrum data can be used to identify the degree of crystallinity. The wave number range of  $850\text{-}1500\text{ cm}^{-1}$  is considered to be highly sensitive to the crystal structure of the cellulose. There are two other peaks considered very important - wave number range of  $1420\text{-}1430\text{ cm}^{-1}$  responsible for  $\text{CH}_2$  scissoring motion and  $893\text{-}897\text{ cm}^{-1}$  responsible for C-H<sub>2</sub> rocking vibrations. According to previously reported literature there are two types of crystallinity indexes called lateral order index (LOI) and total crystallinity index (TCI). The spectral ratio of  $1420/893\text{ cm}^{-1}$  shows the LOI and the spectral ratio  $1375/2900\text{ cm}^{-1}$  gives the TCI (71-73).

In comparison to other samples, MFC-8 that was produced under 56% (w/w) acid concentration, 65 minutes of time and  $80^\circ\text{C}$  temperature shows dominant intensity peaks in fingerprint region that correspond to the cellulose crystalline region. The higher concentration and temperature increased the ability of acid penetration into to a deeper level of the cellular matrix and reacting with the amorphous region of cellulose. It further reduced the size and increased degree of crystallinity of the extracted cellulose.

#### 4.13. Morphology of the MFC

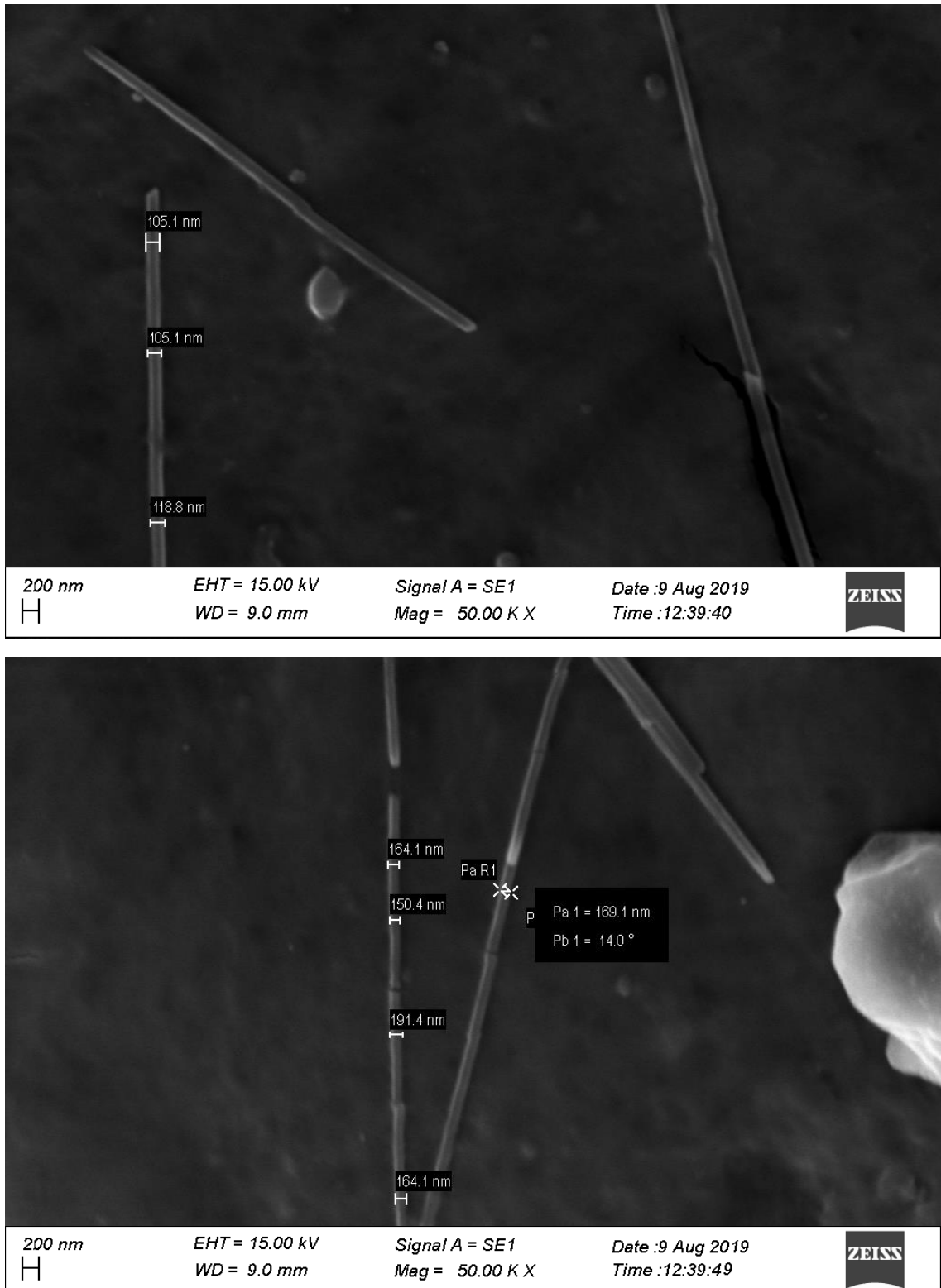


Figure 27: Cellulose fibres of sample MFC 8

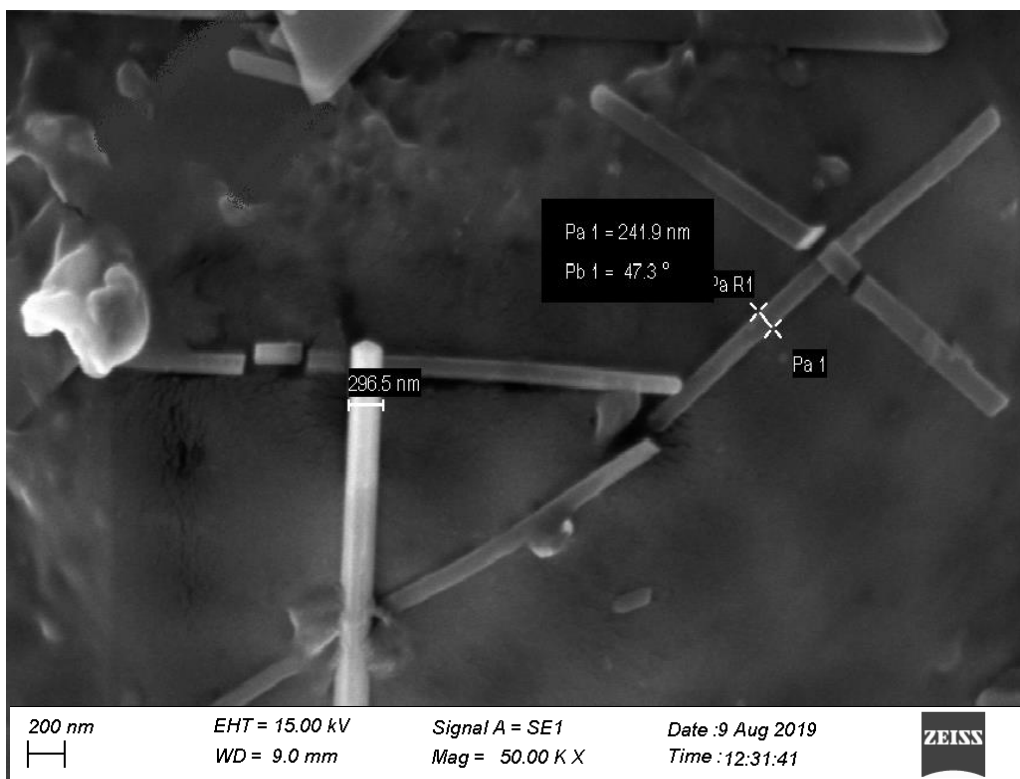
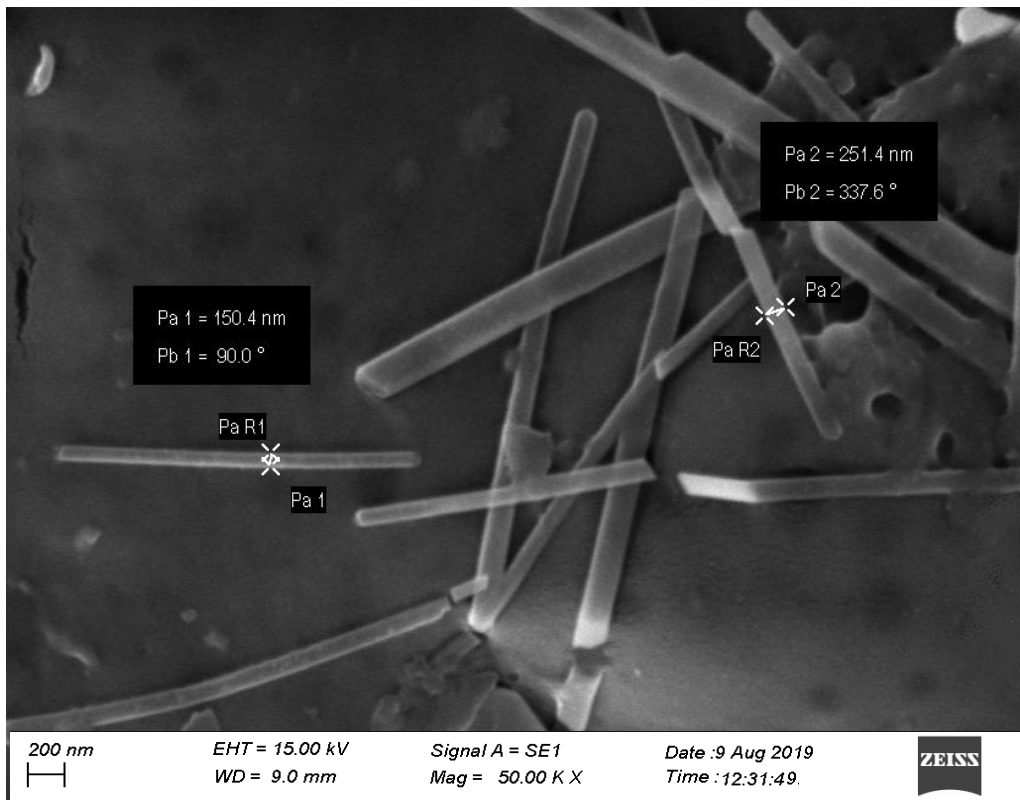


Figure 28: Cellulose fibers of sample MFC-09

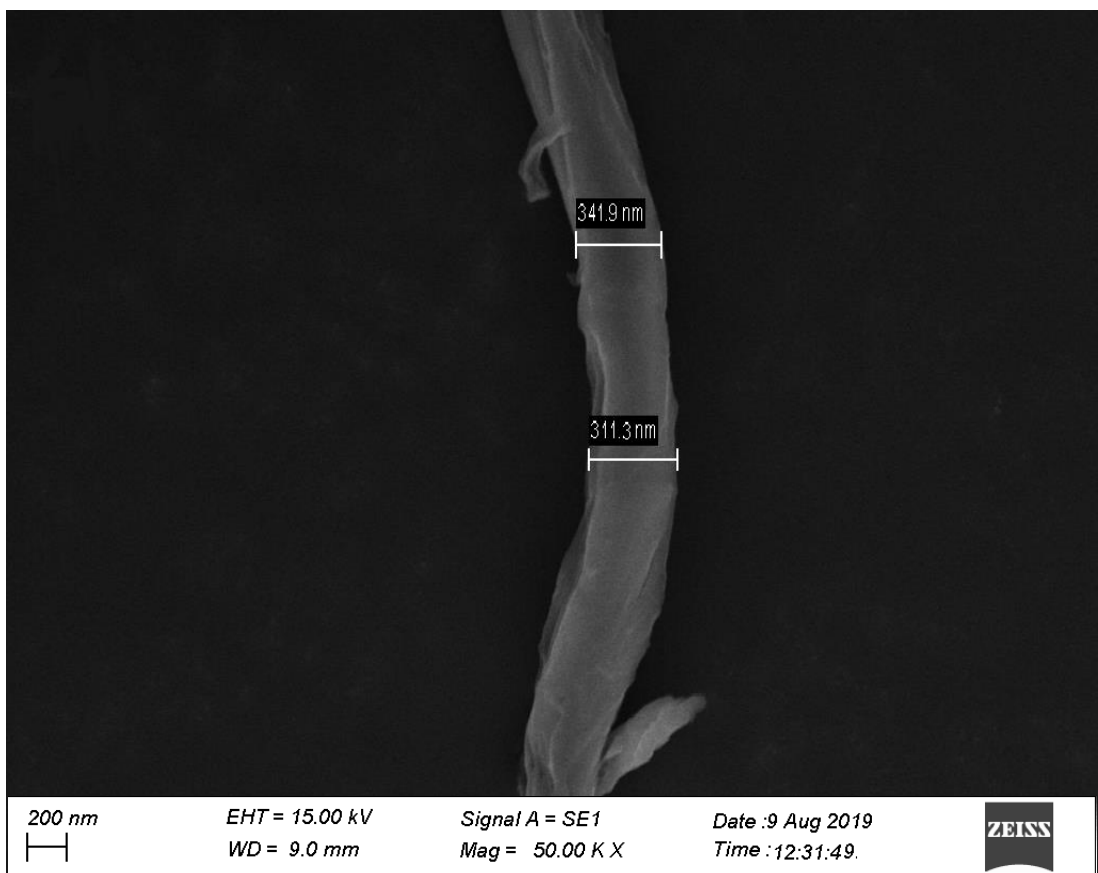
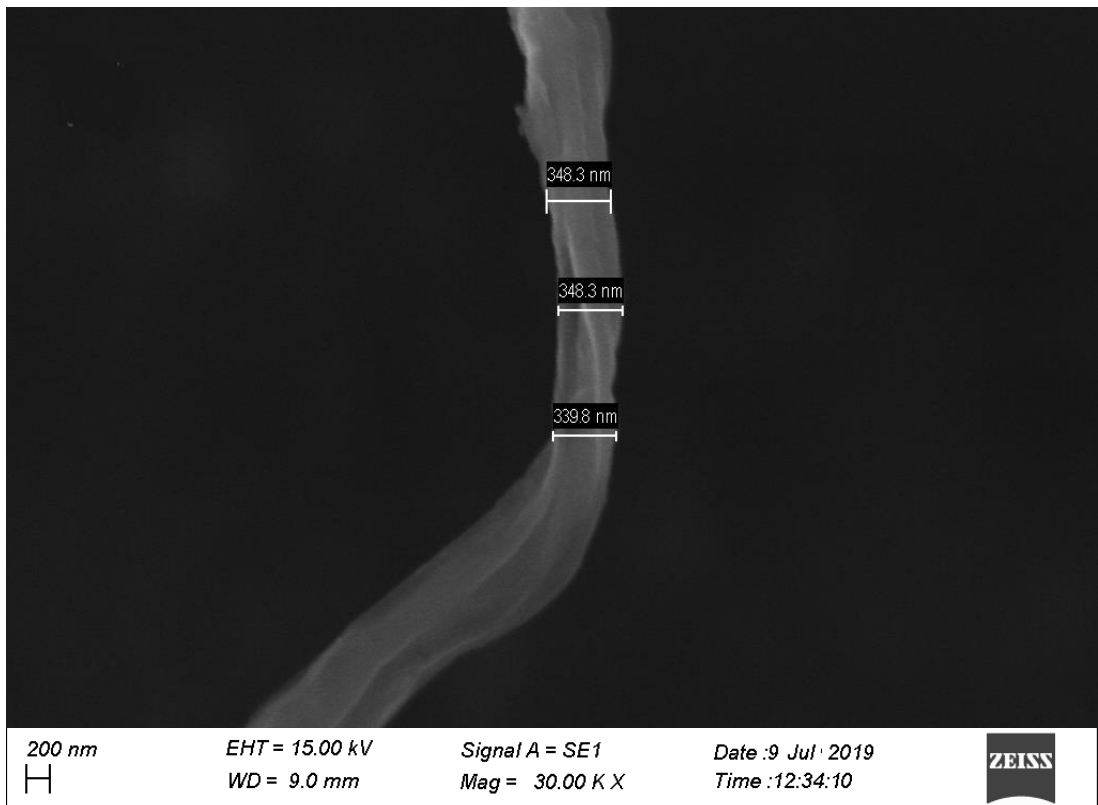


Figure 29: Cellulose fibres of sample MFC 2

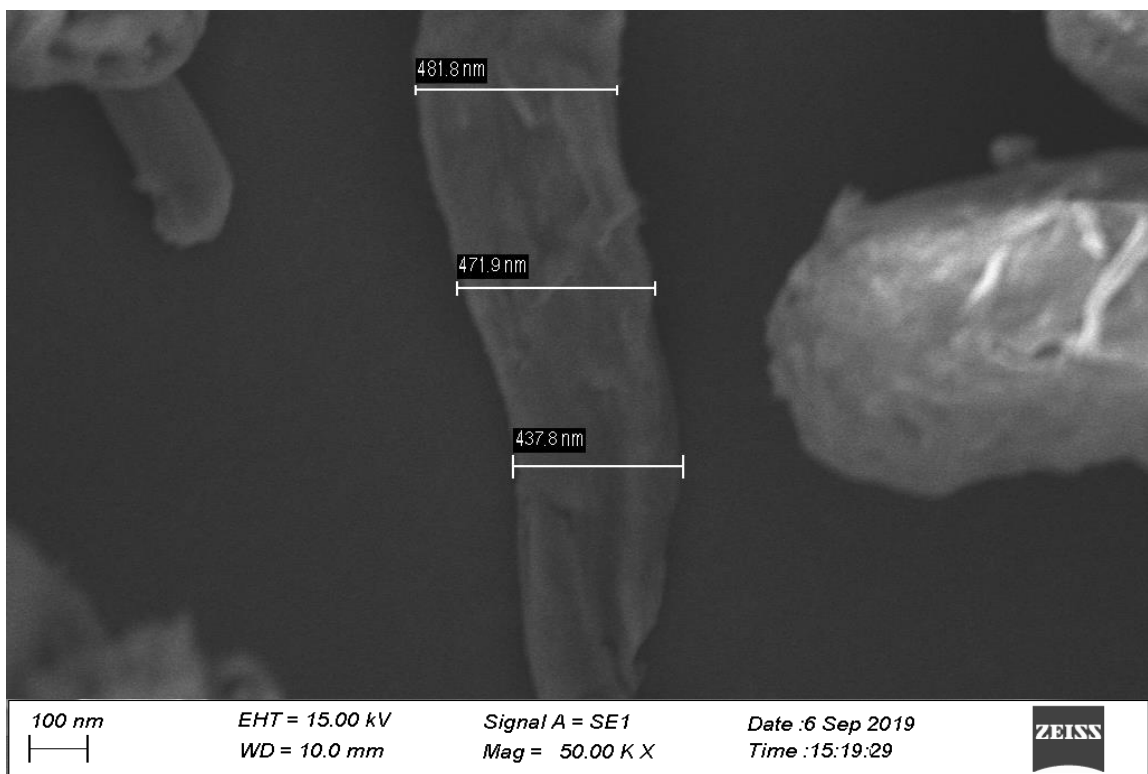
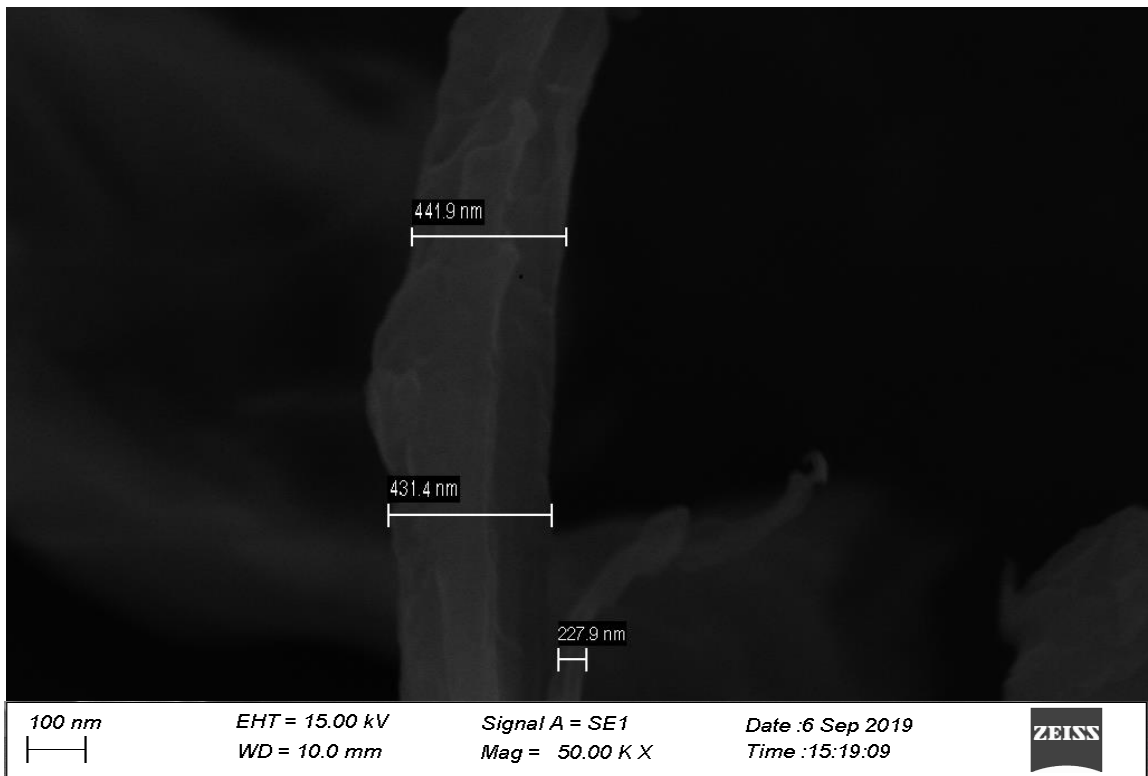


Figure 30: Cellulose fibers of sample MFC 14

In SEM images the different width of the fibres can be clearly observed. The time and the temperature here play a major role in reducing the width of the fibre and the morphology. The surface of the fibres get clearer and smoother when the temperature of the reaction mixture increases.

SEM image of figure no 27 which is more closed to the optimized situation with the mean width of the fibres were shown as 120-160nm and the length was about several microns. Fibre surface was very smooth, clear and straight. High acid concentration and the temperature effectively reduced the width of the fibres. It reveals that the 65 minutes is sufficient to effective acid diffusion in to the cellulose matrix and hydrolysis and high temperature 80<sup>0</sup>C always enhances the diffusing and reaction speed. Here, width and size of fibrils of hydrolysis cellulose was reduced to a great extent due to the removal of all amorphous region of semi-crystalline cellulose.

SEM image of figure no 29, MFC 09 that was kept for nearly 120 minutes shows the diameter range of 150-290 nm with the mean width of 245 nm. The fibres were degraded and the length of the fibres were reduced greatly. This degradation was due to the excess reaction time period. 120 minutes is approximately a doubling of the ideal time period. When the reaction time of the reaction is increased, the fibrillated nature and the high aspect ratio of the cellulose were reduced. When the reaction mixture was kept for a long-time period, the acid penetration in to the matrix is high. Therefore, it was clearly seen that the excess time led to over degradation and tended to break the fibres.

SEM image of figure no 30, MFC 02 shows the fibrillated cellulose with a diameter ranging 300-350nm with a mean value of 340nm. The fibrillated nature of the three-dimensional structure can be clearly observed in this sample. When the reaction time was reduced and the temperature of the reaction mixture is increased, this led to an increase in the width of the cellulose compared to sample no 9. The width of the fibre is high in comparison to the sample MFC-08 and MFC-02 due to insufficient time (10 minutes) to penetrate the polymer matrix. So, in this figure it is evident that the time of the reaction affected the width of the cellulose in the acid hydrolysis process. The rough surface of the MFC was observed due to insufficient time to complete the reaction.

SEM image of figure no 31 shows the MFC in sample MFC-14. The mean width of the fibres is shown as 470 nm and the length is about several microns. The width of the fibre is again increased. The surface of the fibre and the texture of the fibre is mostly similar to the sample MFC-09. When the temperature of the reaction medium was kept at the lower level of 40°C and time at 10 minutes, it again increased the width of the cellulose fibres and yielded a rough surface. When comparing all the samples, it can clearly be seen that to reduce the width of the cellulose, a sufficient amount of temperature and time was needed although the reaction mixture's acid concentration was at the higher levels. The excess time reduced the fibre properties by reducing the length of the fibres.

#### **4.14. Crystallinity of MFC**

Cellulose can be found in nature as varies types including Cellulose I, II, III, and V. Cellulose I is considered as a native cellulose type while Cellulose II are chemically regenerated cellulose usually made in the laboratories. Cellulose I a mixture of two crystalline forms of celluloses  $I_{\alpha}$  and  $I_{\beta}$ . Cellulose  $I_{\alpha}$  has a triclinic crystal system while Cellulose  $I_{\beta}$  has a monoclinic crystal system. The amount of  $I_{\alpha}$  and  $I_{\beta}$  depend on the source of the cellulose [73].

The XRD patterns of the MFC fibres that is extracted from different routines are illustrated in Figure 32. The dominant diffraction peak that is given for cellulose was observed at  $2\theta$  in the ranges between 18° and 21° as the primary peak and a secondary peak are in the range of 10° to 14°. These samples observed at the peaks around  $2\theta = 14.4, 16.6, 18.3$  and  $34.7$  which are correspondent to typical Cellulose  $I_{\beta}$  structure as reported in research literature [73].

Three hydroxyl groups are present in the Cellulose macromolecules. The structure of the cellulose and its physical properties are largely dependent on the hydrogen bonds and the Van der Waals forces. The large number of intramolecular and intermolecular hydrogen bonds determine the crystal structure of cellulose. The hydrogen bonding of the adjacent polysaccharide chain determines the linearity of the cellulose chain and improves the thermal stability and enhances the mechanical



properties. But the hydrogen bonds that form the interchain introduce disorder to cellulose itself. The characteristic peak around  $2\theta = 14.4, 16.6$  reflections gives due to (110) crystallographic plane while peak around  $2\theta = 22.40$  that is assign to the (200) crystallographic plane. Crystallographic plane at the  $22.30-22.40^\circ\text{C}$   $2\theta$  reflection that are responsible for the amorphous domain in the cellulosic matrix. The availability of high amounts of hydroxyl groups in the outer plane of the cellulose causes the occurrence of the most number of interchain and intrachain hydrogen bonds in the (110) crystallographic plane in the cellulose  $I_\alpha$  form [71-73].

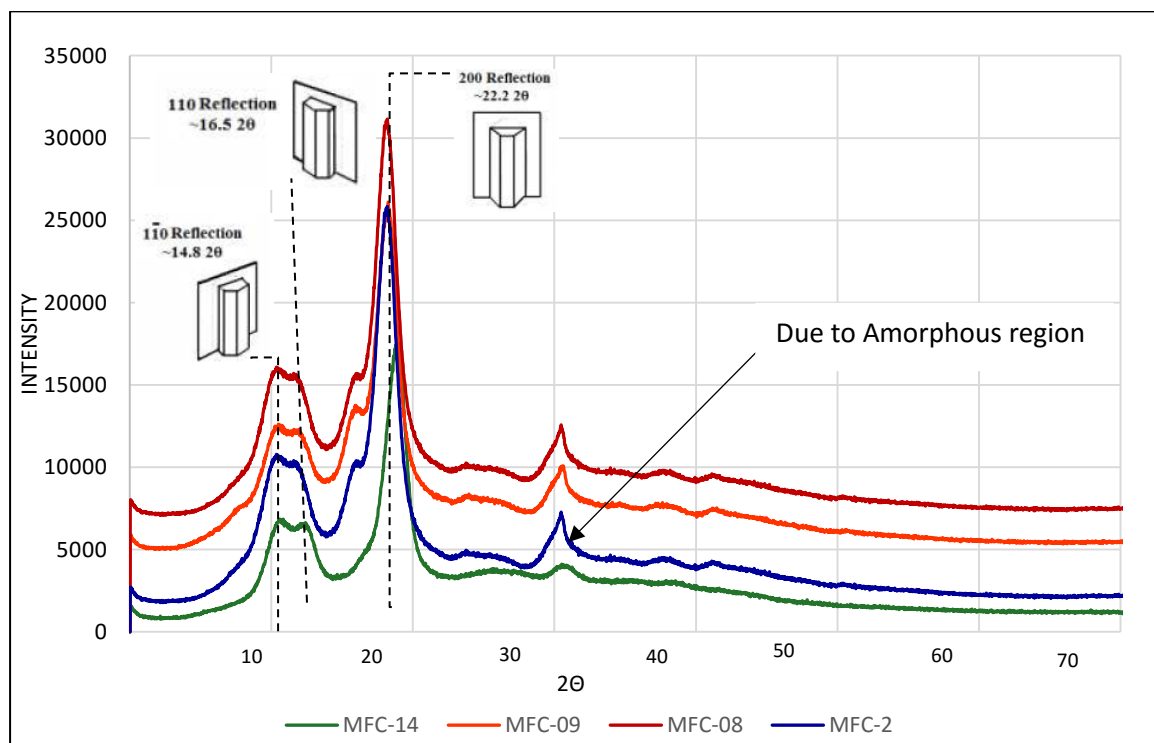


Figure 31: XRD patterns of MFC

When the amount of intrachain hydrogen bonds are high, it forms bond within the (200) crystallographic plan. Intrachain hydrogen bonding is dominant in the cellulose ring bridging O and the neighbouring OH group and is considered a very strong bond and can be usually observed in  $I_\beta$  crystal system. Inter chain hydrogen bonds that are more responsible for the ordered structure of cellulose bonding the other planes (010) and (100) in the Cellulose  $I_\alpha$  triclinic structure and the crystallographic planes of (110) in the Cellulose  $I_\beta$  in monoclinic structure. These bonds bind the

neighbouring cellulose chains together and form Microfibrills. From the XRD distribution pattern, dominant peaks can be observed within the mentioned range for all the MFC samples [71,73].

When comparing all the spectrums MFC-14 is consistent with a more amorphous part than the crystalline domain and recorded a degree of crystallinity as 48%. MFC -02 and the MFC-08 shows higher crystallinity values at 52% and 56% respectively. The degree of crystallinity of the raw cotton fabric is 32%, which is a relatively low crystallinity index value. In acid hydrolysis, most of the amorphous region was discarded, in MFC -08 the degree of crystallinity increased by 24%. A considerably amorphous part remained in the MFC. The degree of crystallinity value of the MFC depends upon the initial source of the material. The cotton fabric's degree of crystallinity value is at a 32% and it contained very high amount of amorphous part although it consisted of a high amount of the cellulose. Apart from that the degree of crystallinity value which depend on the efficiency of the acid hydrolysis process and the effectiveness of penetration of acid that is controlled by the acid hydrolysis temperature and the time. If the dialysis process was not efficiently removed, the unreacted Sulfate that remains in the acid hydrolysis may cause a reduce the degree of the crystallinity index. Table 14 shows the d values or the crystallite sizes along with the three crystallographic planes. The d values of the three crystallographic planes around all the MFC samples shows almost similar values.

Table 14: The crystal structure given band position in  $2\theta^\circ$  and their d-spacing values.

Sample	(110)		(110)		(200)	
	$2\theta$	d (nm)	$2\theta$	d (nm)	$2\theta$	d (nm)
MFC-02	14.03°	5.86912 Å	16.61°	5.45071 Å	22.40°	3.95041 Å
MFC-08	14.04°	5.86906 Å	16.61°	5.45062 Å	22.41°	3.95040 Å
MFC-09	14.02°	5.86952 Å	16.63°	5.45083 Å	22.40°	3.95051 Å
MFC-14	14.02°	5.86991 Å	16.62°	5.45099 Å	22.42°	3.95059 Å

The degree of crystallinity parameter is one of the most important parameter because it gives the information of the rigidity of the cellulose fibres as when the degree of crystallinity increases, the rigidity of the cellulose also increases. When the amorphous part is high the flexibility of the fibre is correspondingly high.

#### 4.15. Thermal degradation behaviour of MFC

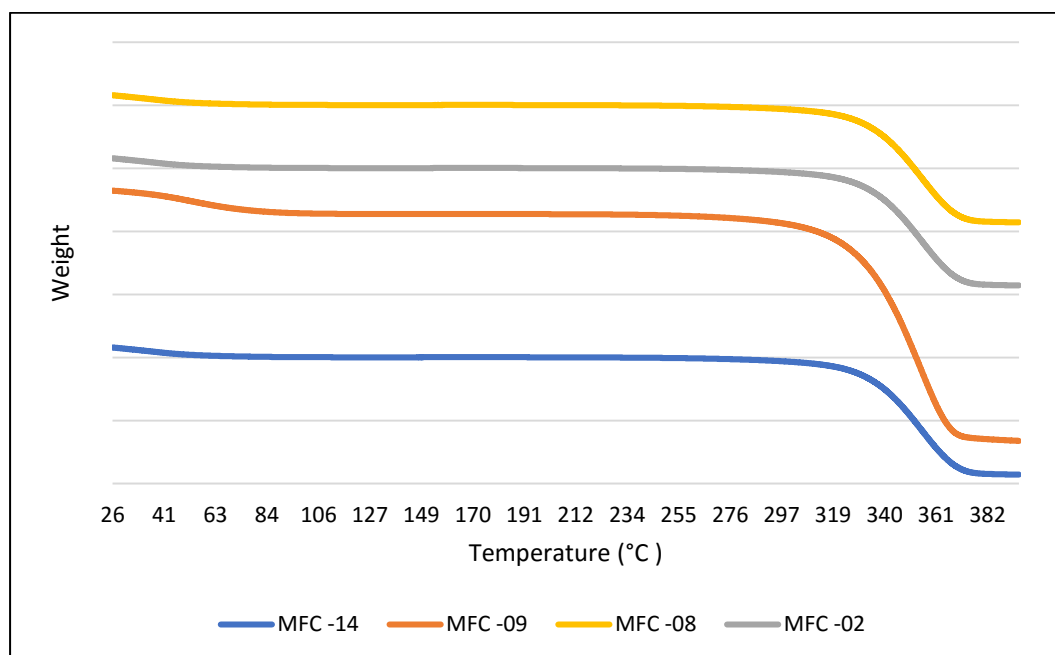


Figure 32: TGA curves of MFC

Figure 33 shows the TGA curves of the Microfibrillated cellulose samples of MFC-02, MFC-08, MFC-09 and MFC-14. The thermal degradation behaviour of the cellulose depends on the inter and intra molecular hydrogen bonding present inside the cellulose matrix. Almost all the TGA curves follow the same pattern of thermal degradation. A lesser amount of weight loss in all 4 MFC samples occurs between 45-65°C that is responsible for the removal of absorbed water and the moisture in cellulose. For the initial step of weight loss of MFC-2, MFC-8, MFC-9 was observed as 5.0% while MFC-14 was 9.1%.

The second step of weight loss is significant. Many studies related to the thermal decomposition of the cellulose can be found in literature. Thermal decomposition of cellulose starts at around 316 °C and the degradation continue up to 400 °C while maximum weight loss can be observed at 315-335 °C. It corresponds to the decomposition of cellulose. Hemicellulose usually starts to decompose at 220°C and remaining up to 315 °C. All the four samples show the characteristic thermal decomposition behaviour around 315-335 °C[71,73].

## 5. Conclusion

Micro fibrillated cellulose was successfully isolated from recycled waste cotton fabric by chemical purification and acid hydrolysis combination with ultrasonication. Chemical purification process of alkali and bleaching treatments give the white colour cotton fibre pulp. The FTIR, XRD and TGA results show the chemically purified cotton fabric fibres possesses properties almost similar to fresh cotton lint.

The properties of MFC is determined by various factors, mainly the source of the cellulose and effectiveness of the acid hydrolysis process [15]. Waste cotton fabric was used as the native cellulose source by considering its availability as waste as well as its low cost. The efficiency of the hydrolysis process can be enhanced by optimizing the hydrolysis parameters including the Sulfuric acid concentration, reaction mixture temperature and reaction time. Three factors were optimized by using Response surface methodology. The developed FTIR second order derivative spectroscopic method was useful to determine the composition of cotton in the cotton/polyester blend.

The sulfuric acid concentration shows the highest effect on the width and the yield of the MFC at 95% confidence intervals. The SEM observations clearly show that when increasing the temperature from 40 °C to 80°C by 40°C the width of the cellulose was reduced by 38%. It requires a sufficient time period for acid penetration into the cellulose matrix at all temperatures. The ANOVA results on the experimental data suggest that the acid concentration and temperature are critical factors on the yield of the cellulose while acid concentration and time are most significant on the width of the cellulose fibres. The regression model for the width and the yield of MFC by cotton fabric are as follows;

$$\text{Mean Width (nm)} = 436.3 - 284.9 \text{ Con.} + 62.1 \text{ Tim} - 20.2 \text{ Tem} - 116.3 \text{ Con}^2 + 109.2 \text{ Tim}^2 + 69.5 \text{ Tem}^2$$

$$\text{Yield\%} = 27.333 - 4.500 \text{ Con.} - 1.500 \text{ Tem} - 2.417 \text{ Con}^2 + 1.083 \text{ Tim}^2 - 1.917 \text{ Tem}^2 - 4.000 \text{ Tim*Tem}$$

The optimized hydrolysis conditions that were given by the model were 56% (w/w) acid concentration, 68-minute hydrolysis time and 70 °C reaction mixture temperature. In practical situations, 140 nm width MFC can be obtained by keeping the sulfuric acid

concentration at 56% (w/w), 80°C temperature and 65 min of reaction time. The length of the MFC was approximately several microns with the yield of 18% by initial weight.

The morphological properties and the dimensions of extracted MFC by different conditions provide valuable information about the acid hydrolysis process. When the temperature is increased from 40 °C to 80 °C, the surface morphology of the MFC changed with a reduction in the diameter of fibres. When the temperature was increased, the fibrillated nature of the three-dimensional fibre reduced greatly and showed smooth surface and increased the straightness. Even though cellulose fibres tend to be aggregated easily, most of the fibres were distributed fairly with very clean surface.

The chemical structure and the degree of crystallinity of MFC were measured using the FTIR and XRD. FTIR spectrums clearly reveal the stable cellulose chemical structure under different reaction conditions in acid hydrolysis. The crystallinity index was determined by the acid concentration and reaction temperature. The highest degree of crystallinity value was obtained at 56%. During the extraction of MFC the crystallinity value was increased from 32%. TGA curve was used to analyse the thermal properties of MFC. Extracted MFC shows characteristic cellulose decomposition at the 315-335 °C. Therefore, this laboratory extracted MFCs can be used as a reinforcing agent, super water absorbing material, composite coating, carbohydrate additive in food industry and various other potential applications with a huge value addition.

## 6. References

1. D. P. Egodage, H. T. S. Jayalath, A. M. P. B. Samarasekara, S. P. A. Madushani, and S. M. N. S. Senerath, "Novel antimicrobial nano coated polypropylene based materials for food packaging systems," in Engineering Research Conference (MERCon), 2017, pp. 88-92.
2. M.P.A. Nanayakkara, W. G. A. Pabasara, A. M. P. B. Samarasekara, D. A. S. Amarasinghe, and L. Karunanayake, "Novel Thermogravimetry Based Analytical Method for Cellulose Yield Prediction of Sri Lankan Rice Straw Varieties," in Moratuwa Engineering Research Conference (MERCon), 2018, pp. 185-190
3. A. M. P. B. Samarasekara, H. D. G. Sumudumalie, and K. H. R. Sajeewani, "Extraction of photo activators using natural resources to develop photodegradable polymer products" in 17th ERU Symposium, 2013.
4. A. M. P. B. Samarasekara and P. Y. Gunapala, "Effect of Papain on the biodegradability of polyethylene modified by Chitosan" in 14th ERU Symposium, 2013.
5. S. Umadaran, P. Somasuntharam, and A. M. P. B. Samarasekara, "Preparation and characterization of cellulose and hemicellulose based degradable composite material using sugarcane waste " presented at the Moratuwa Engineering Research Conference (MERCon), 2016, pp. 367-372.
6. A. M. P. B. Samarasekara, S. A. K. V. M. Piyathilake, and D. I. U. Kumara, " Utilization of fruit waste to produce biodegradable polymer composites," presented at the 17th ERU Symposium, 2013.
7. A. M. P. B. Samarasekara, P. Somasuntharam, and S. Umadaran, "Development of Environmentally Friendly Cellulose Containing Packaging Products From Waste Materials," in Proceedings of the International Postgraduate Research Conference 2015 University of Kelaniya, pp. 184, 2015.
8. A. M. P. B. Samarasekara, H. V. H. H. Senavirathne, and A. H. W. O. Sandaruwan, "Preparation of biodegradable polymer materials using agricultural waste," " in Proceedings of International Forestry and Environment Symposium, vol. 17, 2012, pp. 54.
9. K. D. H. N. Kahawita and A. M. P. B. Samarasekara, "Extraction and characterization of cellulose fibers from sawmill waste," in Moratuwa Engineering Research Conference (MERCon), 2016, pp. 343-348.

10. A. M. P. B. Samarasekara, S. P. D. A. Kumara, A. J. S. Madhusanka, D. A. S. Amarasinghe, & L. Karunanayake, "Study of Thermal and Mechanical Properties of Microcrystalline Cellulose and Nanocrystalline Cellulose Based Thermoplastic Material", in oratuwa Engineering Research Conference (MERCon), 2018, pp. 465-470.
11. A. M. P. B. Samarasekara, A. W. C. Chamikara and W. W. H. P. Wijesundara, "Extraction and Usage of Starch from Banana Pseudostem to Develop Biodegradable Polymer Composites," in in Proceedings of International Forestry and Environment Symposium, vol. 18, 2014.
12. A. M. P. B. Samarasekara. and. E. A. P. C. D. Jayasuriya, "Synthesis of Biodegradable Polyolefins Based Polymer Composites Using Degradable Natural Materials " in in Proceedings of International Forestry and Environment Symposium, vol. 18, 2014, pp. 61.
13. A. M. P. B. Samarasekara, M. D. S. L. Wimalananda, and N. Muthugala, "Utilisation of Photo Activators to Produce of Low Density Polyethylene Based Photodegradable Composite Materials," in Proceedings of International Forestry and Environment Symposium, vol. 18, 2014.
14. D.A.S. Amarasinghe, A. M. P. B. Samarasekara, W.A.D.P. Madhuwanthi, and D.N.S. Dammage, , "Nano-Silver Impregnated Wrapping Film to Keep Fruit Fresh " presented at the Moratuwa Engineering Research Conference (MERCon) 2018, pp. 511-516.
15. M. P. A. Nanayakkara, W. G. A. Pabasara, A. M. P. B. Samarasekara, D. A. S. Amarasinghe, and L. Karunanayake, "Extraction and Characterisation of Cellulose Materials from Sri Lankan Agricultural Waste.," in Proceedings of International Forestry and Environment Symposium, vol. 22, 2017, pp. 47.
16. A. M. P. B. Samarasekara. K. D. H. N. Kahawita, "Extraction and Characterization of Cellulosic Fibers from Sawmill Waste," presented at the 2016 Moratuwa Engineering Research Conference (MERCon), 2016, pp. 343-348..
17. M.P.A. Nanayakkara, W. G. A. Pabasara. A. M. P. B Samarasekara, D. A.S., Amarasinghe and L .Karunanayake, "Synthesis and Characterization of Cellulose from Locally Available Rice Straw," presented at the 2017 Moratuwa Engineering Research Conference (MERCon), 2017, pp. 176-181.

18. A.M.P.B Samarasekara, P. Somasuntharam. a. S. Umadaran. "Development of Environmentally Friendly Cellulose Containing Packaging Products From Waste Materials," in Proceedings of the International Postgraduate Research Conference 2015 University of Kelaniya, 2015, pp. 184.
19. A. M. P. B. Samarasekara, J. D. C. M. Jayakody. and A. G. S. Madurasangani, "Study and development of low density polyethylene (LDPE) based biodegradable polymer materials using Kitul flour," in Proceedings of International Forestry and Environment Symposium , vol. 17, 2012,pp. 41.
20. Beck-Candanedo, S., Roman, M., and Gray, D. G., "Effect of reaction conditions on the properties and behavior of wood cellulose nanocrystal suspensions", *Biomacromolecules*, 6, 1048- 1054, 2005.
21. Anuj Kumar , Yuvraj Singh Negi, Veena Choudhary , Nishi Kant Bhardwaj. "Characterization of Cellulose Nanocrystals Produced by Acid-Hydrolysis from Sugarcane Bagasse as Agro-Waste". *Journal of materials physics and chemistry*, 1-8,vol 2,2014.
22. Chang and Chih-Ping. "Preparation and Characterization of Nanocrystalline Cellulose by Acid Hydrolysis of Cotton Linter".*Taiwan Journal of Forest Science*, vol.25,pp.231-244,,2013.K. D. H. N. Kahawita, A. M. P. B. Samarasekara, D. A. S. Amarasinghe, & L. Karunanayake, "Fabrication of Nanofibrillated Cellulose (NFC) Based Composite Materials for Engineering Applications", in Proceedings of International Forestry & Environment Symposium, 2018.
23. P. Y. Gunapala and A. M. P. B. Samarasekara, "Extraction and modification of chitosan from fishery waste to develop biodegradable polyethylene films," in 12th ERU Symposium, pp. 38-39, 2013.
24. D.P.Egodage, H.T.S Jayalath, A.M.P.B Samarasekara and D.A.S. Amarasinghe, "Preparation of Nano Silver Based Antibacterial Coating for Food Packaging Applications", in Annual Transactions of Institution of Engineers Sri Lanka, 2016, pp 165-170.
25. L.D Rajapaksha, H. A. D. Saumyadi. A.M.P.B Samarasekara, D.A.S Amarasinghe and L .Karunanayake, "Development of Cellulose Based Light Weight Polymer Composites," presented at the 2017 Moratuwa Engineering Research Conference (MERCon), 2017, pp. 186-186.



26. A. M. P. B Samarasekara, K. D. H. N. Kahavita. D. A.S.,Amarasinghe and L .Karunanayake, "Fabrication and Characterization of Nanofibrillated Cellulose (NFC) Reinforced polymer composite," presented at the 2018 Moratuwa Engineering Research Conference (MERCon), 2018, pp. 449-454.
27. A. M. P. B. Samarasekara, J. D. C. M. Jayakody, and A. G. S. Madurasangani, "Zingibain-Pectin LDPE as a biodegradable composite material," in Proceedings of International Polymer Science and Technology Symposium, vol. 1, 2012.
28. H.P.S. Abdul Khalil \*, A.H. Bhat, A.F. Ireana Yusra, "Green composites from sustainable cellulose nanofibrils: A review", Journal of Carbohydrate polymers 87, 963-979, 2012.
29. Mohanty, A. K., Misra, M., & Drzal, L. T, "Sustainable Bio-Composites from renewable resources: Opportunities and challenges in the green materials world", Journal of Polymers and the Environment, 10(1-2), pp19-26, 2002.
30. Wenshuai Chen, "Individualization of cellulose nanofibers from wood using high-intensity ultrasonication combined with chemical pretreatments", Volume 83, Issue 4, pp Pages 1804-1811, 1 February 2011.
31. Ouchi, A., Toida, T., Kumaresan, S. et al. A new methodology to recycle polyester from fabric blends with cellulose. Cellulose 17, 215–222, 2010.
32. G. M. EI-Nouby, H. A. Azzam, S. T. Mohamed, and M. N. El-Sheikh, "Textile Waste-Material Recycling, Part I: Ways and Means, Textile Processing: State of the Art & Future Developments", Vol. 2, pp.394–407, 2nd International Conference of Textile Research Division, NRC, Cairo, Egypt, April 11–13, 2005.
33. Muthu, S.S., Li, Y., Hu, J.Y. et al. Carbon footprint reduction in the textile process chain: Recycling of textile materials. Fibers Polym 13, 1065–1070, 2012.
34. F. orhan and A. Durand "Quantitative Analysis of Cotton–Polyester Textile Blends from Near-Infrared Spectra", Applied Spectroscopy 60(5):539-44, June 2006.
35. Azizi Samir MAS, Alloin F, Dufresne A. "Review of recent research into cellulosic whiskers, their properties and their application in nanocomposite field".Biomacromolecules; 6, 612. PMID 2005.

36. Silva GG, Souza DA, Machado JC, Hourston DJ, “Mechanical and thermal characterization of native Brazilian Coir fiber”, *J.Appl.Polym.Sci*, 76, pp 119. 2000.
37. Fan Y, Saito T, Isogai A.” TEMPO-mediated oxidation of b-chitin to prepare individual nanofibrils.*Carbohydr*”, *Polymer*, pp 77, 832 2009.
38. Rosa MF, Medeiros ES, Malmonge JA, Gregorski KS, Wood DF, Mattoso LHC, et al.”Cellulose nanowhiskers from coconut husk fibers”, Effect of preparation conditions on their thermal and morphological behavior.*Polymer*, pp 81, 83 2010.
39. Eichhorn, S. J., Dufresne, A., Aranguren, M., Marcovich, N.E., Capadona, J. R., Rowan, S. J., Weder, C., Thielemans, W., Roman, M., Renneckar, S., Gindl, W., Veigel, S., Keckes, J., Yano, H., Abe, K., Nogi, M., Nakagaito, A.N., Mangalam, A., Simonsen, J., Benight, A. S., Bismarck, A., Berglund, L.A., and Peijs, T., “Review: Current international research into cellulose nano nanofibres and nanocomposites”, *J. Mater. Sci.*, 45, 1-33, 2010.
40. Pandey, J. K., Ahn, S. H., Lee, C. S., Mohanty, A. K., and Misra, M., “Recent advances in the application of natural fiber based composites”, *Macromol. Mater. Eng.*, 295, 975-989, 2010.
41. H.P.S. Abdul Khalil \*, A.H. Bhat, A.F. Ireana Yusra (2012). “Green composites from sustainable cellulose nanofibrils: A review”, *Journal of Carbohydrate polymers* 87, 963-979.
42. Mohanty, A. K., Misra, M., & Drzal, L. T(2002). “Sustainable Bio-Composites from renewable resources: Opportunities and challenges in the green materials world”, *Journal of Polymers and the Environment*, 10(1-2), pp19-26.
43. Wenshuai Chen. (2011). “Individualization of cellulose nanofibers from wood using high-intensity ultrasonication combined with chemical pretreatments”, *Volume 83, Issue 4*, pp Pages 1804-1811.
44. Azizi Samir MAS, Alloin F, Dufresne (2000). “Review of recent research into cellulosic whiskers, their properties and their application in nanocomposite field”.*Biomacromolecules*; 6, 612. PMID.
45. Hult EL, Larsson PT, Iversen T. (2000). A comparative CP/MAS 13C NMR study of cellulose structure in spruce wood and Kraft pulp.*Cellulose*, pp7, 35.
46. Hult EL, Larsson PT, Iversen T (2001). “Cellulose fibril aggregation—an inherent property of kraft pulps”.*Polymer*, pp 42, 3309.

47. Silva GG, Souza DA, Machado JC, Hourston DJ. (2000) “Mechanical and thermal characterization of native Brazilian Coir fiber”, *J.Appl.Polym.Sci*, 76, pp 119.
48. Fan Y, Saito T, Isogai A. (2009) “TEMPO-mediated oxidation of b-chitin to prepare individual nanofibrils. *Carbohydr*”, *Polymer*, pp 77, 832.
49. Eichhorn, S. J., Dufresne, A., Aranguren, M., Marcovich, N.E., Capadona, J. R., Rowan, S. J., Weder, C., Thielemans, W., Roman, M., Renneckar, S., Gindl, W., Veigel, S., Keckes, J., Yano, H., Abe, K., Nogi, M., Nakagaito, A.N., Mangalam, A., Simonsen, J., Benight, A. S., Bismarck, A., Berglund, L.A., and Peijs, T. (2010) “Review: Current international research into cellulose nano nanofibres and nanocomposites”, *J. Mater. Sci.*, 45, 1-33.
50. De Silva, R., Byrne, N. Utilization of cotton waste for regenerated cellulose fibres: influence of degree of polymerization on mechanical properties. *Carbohydrate Polymers*, 174, 89-94: 2017
51. Vaeck, S. V. Chemical and Mechanical Wear of Cotton Fabric in Laundering. *Journal of the Society of Dyers and Colourists*, 82(10), 374-379. doi: 10.1111/j.1478- 4408. 1966.tb 02684: 1966.
52. Beck-Candanedo, S., Roman, M., and Gray, D. G. (2005) “Effect of reaction conditions on the properties and behavior of wood cellulose nanocrystal suspensions”, *Biomacromolecules*, 6, 1048- 1054.
53. Pandey, J. K., Ahn, S. H., Lee, C. S., Mohanty, A. K., and Misra, M. (2010), “Recent advances in the application of natural fiber based composites”, *Macromol. Mater. Eng.*, 295, 975-989.
54. Bondeson D, Mathew A, Oksman K (2006) Optimization of the isolation of nanocrystals from microcrystalline cellulose by acid hydrolysis. *Cellulose* 13(2):171–180
55. Brinchi L, Cotana F, Fortunati E, Kenny JM (2013) Production of nanocrystalline cellulose from lignocellulosic biomass: technology and applications. *Carbohydr Polym* 94(1):154–169
56. Cha R, He Z, Ni Y (2012) Preparation and characterization of thermal/pH-sensitive hydrogel from carboxylated nanocrystalline cellulose. *Carbohydr Polym* 88(2):713–718
57. Chen W, Yu H, Liu Y (2011a) Preparation of millimeter-long cellulose I nanofibers with diameters of 30–80 nm from bamboo fibers. *Carbohydr Polym* 86(2):453–461.

58. Deepa B, Abraham E, Cherian BM, Bismarck A, Blaker JJ, Pothan LA, Leao AL, de Souza SF, Kottaisamy M (2011) Structure, morphology and thermal characteristics of banana nano fibers obtained by steam explosion. *Bioresour Technol* 102(2):1988–1997.
59. Deniz B and Ismail H. “Modeling and optimization I: Usability of response surface methodology”. *Journal of Food Engineering*, vol.78, pp.836-845, Nov .2007.
60. Deniz B and Ismail H. “Modeling and optimization I: Usability of response surface methodology”. *Journal of Food Engineering*, vol.78, pp.836-845, Nov .2007.
61. Chang and Chih-Ping. “Preparation and Characterization of Nanocrystalline Cellulose by Acid Hydrolysis of Cotton Linter”. *Taiwan Journal of Forest Science*, vol.25, pp.231-244, March.2013.
62. D. Bondeson, A. Mathew and K. Oksman. “Optimization of the isolation of nanocrystals from microcrystalline cellulose by acid hydrolysis”. *Cellulose*, vol.13, pp.171-180, Feb.2006.
63. Bondeson, Daniel, Aji Mathew, and Kristiina Oksman. "Optimization of the isolation of nanocrystals from microcrystalline cellulose by acid hydrolysis." *Cellulose* 13.2 (2006): 171.
64. Chang, Chih-Ping, et al. "Preparation and characterization of nanocrystalline cellulose by acid hydrolysis of cotton linter." *Taiwan Journal for Science* 25.3 (2010): 251-64.
65. Kargarzadeh, Hanieh, et al. "Methods for extraction of nanocellulose from various sources." *Handbook of nanocellulose and cellulose nanocomposites 1* (2017): 1-51.
66. Cao, J., Zhang, X., Wu, X., Wang, S. and Lu, C. (2016). Cellulose nanocrystals mediated assembly of graphene in rubber composites for chemical sensing applications. *Carbohydrate polymers*. 140, 88-95.
67. Dufresne, A. (2013). Nanocellulose: a new ageless bionanomaterial. *Materials Today*, 16, 220-227. Fan, M., Dai, D. and Huang, B. (2012). Fourier transform infrared spectroscopy for natural fibres. *Fourier transform-materials analysis*. 3, 45-68.

68. Quantitative Analysis of Cotton–Polyester Textile Blends from Near-Infrared Spectra, *Applied Spectroscopy* 60(5):539-44
69. Kalia, S., Kaith, B.S. and Kaur, I. (2009). Pretreatments of natural fibers and their application as reinforcing material in polymer composites—A review. *Polymer Engineering and Science*. 4,1253–1272.
70. Khalil, H. A., Davoudpour, Y., Islam, M. N., Mustapha, A., Sudesh, K., Dungani, R. and Jawaid, M. (2014). Production and modification of nanofibrillated cellulose using various mechanical processes: a review. *Carbohydrate polymers*. 99, 649-665. Kumar, A., Negi Y.S. and Choudhary, V. (2014).
71. Characterization of Cellulose Nanocrystals Produced by Acid-Hydrolysis from Sugarcane Bagasse as Agro-Waste. *Journal of Materials Physics and Chemistry*. 2, 1-8. Lee, H.V., Hamid, S.B.A. and Zain, S.K. (2014).
72. Conversion of Lignocellulosic Biomass to Nanocellulose: Structure and Chemical Process. *The Scientific World Journal*. 1-20.
73. Poletto, M., Pistor, V. and Zattera, A. J. (2013). Structural characteristics and thermal properties of native cellulose. *Cellulosefundamental aspects*. 2, 45-68.